Fermi National Accelerator Laboratory

FERMILAB-Conf-87/51
2021.000

Experimental Search for *W/Z* Pairs and Higgs Bosons at Very High Energy Hadron-Hadron Colliders*

George Alverson
Northeastern University, Boston, MA 02115

Hans-Uno Bengtsson
University of California, Los Angeles, Los Angeles, CA 90024

John Hauptman
Iowa State University/Ames Laboratory, Ames IA 50010

David Hedin
State University of New York at Stony Brook, Stony Brook, NY 11794

Maria Jose Herrero and Edward Wang
Lawrence Berkeley Laboratory, Berkeley, CA 94720

Stephan Linn and Christopher Young
SCRI and Florida State University, Tallahassee, FL 32306

Barrett Milliken
California Institute of Technology, Pasadena, CA 91125

Frank Paige and Serban Protopopescu
Brookhaven National Laboratory Upton, NY 11973

Aurore Savoy-Navarro†
CEN Saclay, Gif-sur-Yvette CEDEX, France

Torbjörn Sjöstrand
University of Lund, Lund, Sweden

Wesley Smith
Columbia University, New York, NY 10027

Yoshi Takaiwa and Aki Yamashita
University of Tsukuba, Ibaraki, Japan, and Fermi National Accelerator Laboratory, Batavia, IL 60510

March 1987

*To be published in the Proceedings of the 1986 Snowmass Summer Study on the Physics of the SSC, Snowmass, CO, June 23-July 11, 1986.

†Coordinator of the Working Group on "W/Z Pairs and Higgs at the SSC" with J. Gunion.

Operated by Universities Research Association Inc. under contract with the United States Department of Energy

EXPERIMENTAL SEARCH FOR W/Z PAIRS AND HIGGS BOSONS AT VERY HIGH ENERGY HADRON-HADRON COLLIDERS

George Alverson, Northeastern University , Boston MA
Hans-Uno Bengtsson, UCLA, Los Angeles CA
John Hauptman, Iowa State University/Ames Laboratory, Ames IO
David Hedin, State University of New York, Stony Brook NY
Maria Jose Herrero and Edward Wang, Lawrence Berkeley Laboratory, Berkeley CA
Stephan Linn and Christopher Young, SCRI and Florida State University, Tallahassee FL
Barrett Milliken, California Institute of Technology, Pasadena CA
Frank Paige and Serban Protopopescu, BNL, Upton NY
Aurore Savoy-Navarro, CEN Saclay, Gif-sur-Yvette CEDEX France
Torbjörn Sjöstrand, University of Lund, Lund Sweden
Wesley Smith, Columbia University, New York NY
Yoshi Takaiwa and Aki Yamashita, Tsukuba University/Fermilab, Batavia IL

Abstract

We study, from an experimental point of view, the main ways to detect standard high mass Higgs bosons (from 300 Gev up to about 1 TeV) when they decay into W- and Z-pairs at the SSC. We also consider the corresponding W- and Z^0-pair continuum which may itself provide interesting physics, and we pay some attention to the case of an intermediate mass charged Higgs decaying into $\tau\nu_\tau$ ($m_{H^\pm}$=300 GeV). We first explain why and how high energy pp colliders may search for Higgs' and we compare their possible performances to those of the e^+e^- and ep colliders at all possible mass scale (from few tens of GeV's up to 1 TeV). We then estimate the rates of the signals and the main backgrounds. We define the main characteristics of these events as reproduced by M.C. generators (especially implemented with these processes) and simulated through an idealized 4π fine-grained calorimeter. A trigger strategy for W- and Z-pairs is derived from this study.

1.Introduction

Since the first run of the CERN $p\bar{p}$ collider in June 1981, experimentalists have been able to explore the W-mass range extending from a few tens of Gev to of the order of 100 Gev. The first goal achieved was the discovery[1] of the Intermediate Vector Bosons (IVB's): the W and the Z^0. The UA1 and UA2 experiments have studied the properties of the IVB's and verified the main predictions of the Glashow-Weinberg-Salam model. In addition, a wide variety of unexplained events have been observed which include jet(s) and/or lepton(s) and/or missing energy. Even if these events are well described, at the present time,[2] by the standard model, they show that the present experiments will be able to look for new signals if provided with upgraded detectors and higher beam energy and/or higher luminosity. Therefore, the results obtained by the first generation of detectors at the CERN $p\bar{p}$ collider have generated a lot of hope and enthusiasm for hadron hadron colliders. A new set of machines at or above the Z^0 mass threshold will start to run within the next year: Tevatron, SLC, and ACOL. ACOL at

CERN will increase the integrated luminosity obtained so far by about a factor of ten. The Tevatron at FNAL will provide $p\bar{p}$ interactions at $\sqrt{s} \approx 2$ TeV. SLC should give e^+e^- interactions at $\sqrt{s} = 90$ GeV in 1987. LEP phase I should start to work by 1989. Both the Tevatron and LEP have foreseen improvements somewhere around 1992. The scheduled upgrades are increased luminosity of the order of $5 \times 10^{31}\text{cm}^{-2}\text{s}^{-1}$ at FNAL and increased energy at LEP II to $\sqrt{s} = 130\ GeV$. These new machines and their associated detectors will allow study of the details of physics above the 100 GeV scale. Since the W-pair production threshold will be crossed, the investigation of the "Higgs sector" can begin.

So far we know very little about the Higgs particle. Consistency of the standard model requires the existence of a scalar boson, the minimal Higgs, which is the inseparable comrade of the W and Z^0. So at first glance nothing about it seems strange; it is just "standard". Despite this friendly appearance, the Higgs has some disturbing theoretical and experimental aspects. Its mass is loosely constrained to be between a few GeV and $\approx$1 TeV. Therefore, it is not easy for experimentalists to search for it. The existence of the Higgs is the cause of the so-called hierarchy problem, which is unsolved by the standard model. Only Supersymmetry (SUSY) has succeeded in resolving it in an elegant, but expensive, way. In any case, the Higgs is inevitably related to the existence of a threshold for new physics. This threshold should naturally be at around 1 TeV if there is no "Desert".

The existence of W's and Z^0's has been proven by the experimentalists, and the standard model has been shown,so far, to be accurate at the 5 percent level. The next clear goal is to learn more about the Higgs sector. Searching for IVB pairs and Higgs bosons is one of the main tasks, if not the main task, of the next generation(s) of machines, detectors, and experimentalists.

This report will concentrate on how to detect such objects, especially when they are massive ($m_H > 2m_W$). We start, in Section 2, by trying to answer the question: "why and how does one look for Higgs at a pp collider?" We compare the possibilities of this machine with those of e^+e^- and ep colliders. Two cases are discussed: First, one considers the hypothesis of a low mass Higgs ($m_H < 2m_W$). We examine the capabilities of the Tevatron with luminosity $10^{30}\text{cm}^{-2}\text{s}^{-1}$ and $5 \times 10^{31}\text{cm}^{-2}\text{s}^{-1}$. Also a 10-18 TeV pp machine is investigated. A comparison with LEP I, SLC, LEP II and LEP200 is done. Second, one then consideres the case of a massive Higgs ($m_H > 2m_W$). This subsection contains a description of the processes and their main features that are relevant for the SSC. It also includes a discussion of the intermediate mass case (i.e. $m_{H^0} = 2m_W$) where it is shown that super ep-colliders could have a relevant contribution. Section 3 summarizes a study of the rates of the signals and their corresponding backgrounds which may be expected for the various scenarios considered at the SSC. In Section 4, we describe the main characteristics of the events and define a trigger strategy. A second report * focuses on the main detection issues which have to be faced when searching for IVB pairs and Higgs' at the SSC. This includes the problems of identifying W's and Z^0's decaying into leptonic or hadronic modes, of searching for purely leptonic signatures of the Higgs and the continuum, and also an estimate of the confusion due to the pile-up of events. We have tried, for each of these topics, to examine from an experimental point of view various aspects of detectors and their respective sensitivities to physically relevant observables. In the conclusion we define main features of a detector able to "realistically" perform such a search, estimate the overall efficiency for each case and, finally, compare the various scenarios we have envisioned and confront their feasibilities.

2. The Search for Higgs Bosons at PP Colliders: Why and How

Before discussing the search for Higgs bosons at very high energy pp machines, it is worthwhile to summarize the capabilities of present and future hadron hadron colliders and to compare them to other machines (e^+e^- and ep colliders). The mass range where different machines are able to search for the Higgs is naturally divided into three regions by the scale factor m_W. The "low mass" Higgs lies in the range from a few GeV $< m_{H^0} < m_W$. An "intermediate mass" Higgs would have mass is between m_W and $2m_W$. Finally, we suppose that the Higgs mass is greater than $2m_W$ and can extend up to $\approx$1 TeV; this is a "high mass" Higgs. These three scenarios are quite different in many respects; however, we will show that in each case pp colliders can make significant contributions.

2.1 Low Mass Higgs

If the minimal Higgs exists and has a mass less than the W it is certainly the e^+e^- colliders which will have the best chance to discover it. However, despite the strong competition, the Tevatron and higher energy colliders may also contribute very actively to this search.

2.1.1 Low Mass Higgs and e^+e^- Colliders

In 1987, Tristan and SLC will begin working. The SLC will operate at around $\sqrt{s} = 90\ GeV$. At the beginning of 1989, LEP will turn-on and, from 1990 till 1992, the c.m. energy of this machine will be slowly increased up to about 130 GeV at LEP phase II. Due to these machines, very low mass Higgs bosons up to 30 GeV or at most 40 GeV could be discovered. The extension of LEP up to 200 GeV[3] would have a good chance of discovering a Higgs up to masses of 80 GeV. A recent study[4] considered a peaked luminosity of $10^{31}\text{cm}^{-2}\text{s}^{-1}$ (1 pb^{-1} per day) at $\sqrt{s} = 200$ GeV. The computed rates correspond to an integrated luminosity of 500 pb^{-1} (2 or 3 years of running). The reaction studied was:

$$e^+e^- \rightarrow H^0 + Z^0 \qquad (2-1),$$

and the main corrsponding backgrounds are

$$e^+e^- \rightarrow W^+W^- \text{ or } Z^0Z^0$$

and

$$e^+e^- \rightarrow q\bar{q}, q\bar{q}g, ...$$

The rates for this case, as well as the calculated detector efficiencies, are summarized in Table 2.1. It essentially shows that above 80 GeV the cross-section of process 2.1 becomes too low and the backgrounds become quite severe. The case where $m_{H^0} \approx 90\ GeV$ is difficult due to the Z^0 background. If $m_{H^0} \approx 100\ GeV$, the rate is quite low (100 events for 500 pb^{-1}) but should be feasible with a sophisticated analysis. Although these results are certainly preliminary, they show that if the Higgs is in the mass range from 40 to 80 GeV an e^+e^- collider should not miss it.

• This second report is: *Detecting W/Z Pairs and Higgs at High Energy pp Colliders: Main Experimental Issues*, by G. Alverson *et al.*, FNAL-CONF-87/54 and to be published in the Proceedings of the 1986 Snowmass Summer Study on the Physics at the SSC, Snowmass, Colorado, June 23-July 11, 1986.

TABLE 2.1

Estimated rates for H^0 production at LEP200 with ϵ being the reconstruction efficiency and S/B being the signal to background ratio (see reference 4).

Decay modes	m_{H^0} (GeV)	Rate (500pb^{-1})	ϵ	S/B
$H^0Z^0 \to (b\bar{b})(\nu\bar{\nu})$	40	107	.47	17
	60	83	.41	4
	80	55	.22	4
$e^+e^- \to H^0Z^0$	40	36	.67	Large
$H^0 \to b\bar{b}$	60	28	.60	28
$Z^0 \to e^+e^-, \mu^+\mu^-, \tau^+\tau^-$	80	18	.61	4
$H^0 \to b\bar{b}$ jets	40	430	.18	3
$Z^0 \to q\bar{q}$ jets	60	340	.18	2

2.1.2 Low Mass Higgs and pp Colliders

In early 1987, the Tevatron at FNAL utilizing the CDF detector will begin to operate at $\sqrt{s} = 1.8\ TeV$ and a peak luminosity of $10^{29}\text{cm}^{-2}\text{s}^{-1}$ (10^{36}cm^{-2} per year). The nominal value of the luminosity is forseen to increase to 10^{30} in the second or third year of operation with a proposed upgrade giving 5×10^{31} in about 1992. Despite the common statement that e^+e^- colliders are the best place to look for Higgs bosons in this mass range, we have initiated a study[5] to investigate how pp colliders can participate in this search.

For Higgs masses below the t-quark mass, decays into $\tau^+\tau^-$, $c\bar{c}$ and $b\bar{b}$ are the most important as $\tau^+\tau^-$ gives the cleanest signature and $b\bar{b}$ is the dominant[6] decay mode. Above twice the t-quark mass the $t\bar{t}$ decay mode dominates. For low mass Higgs' produced at pp colliders, we will mainly consider its decay mode into $\tau^+\tau^-$, where $\tau \to \pi\nu_\tau\pi^{0\prime}s$. This is so far the best way to identify H^0's. The two jet case (produced by $H^0 \to b\bar{b}$), which is the preferred process in e^+e^-, has to overcome a huge and very difficult QCD background. The only way to deal with such relatively low E_t jets would be to identify b's (as of now, no microvertex detector has worked in a pp collider enviroment). Moreover, the beam jets would add to the confusion in the event.

We have studied how the Tevatron $p\bar{p}$ collider with $\sqrt{s} = 2\ TeV$ or a pp collider with 10-18 TeV would search for such low mass H^0's. The main way to produce such objects at these energies is through the qq or gg fusion mechanism; WW and Z^0Z^0 fusion are much smaller in this case by a factor greater than ten. Another production mechanism is via hadroproduction process:

$$u\bar{d} \to W \to WH^0$$

and

$$u\bar{u} \to Z^0 \to Z^0H^0.$$

These processes are also lower than the dominant process by a factor of ten; but it produces an interesting signature if one looks at the decay of W into $q\bar{q}$ or Z^0 into $\nu\bar{\nu}$. Various scenarios of low mass Higgs' at $p\bar{p}$ colliders using the Pythia Monte Carlo[7] have

been generated . The generated events have then been submitted to the full simulation package of the CDF experiment.[8] We have estimated the rates for each studied case and scanned in detail the CDF displays of the simulated events and have started to estimate the backgrounds. The largest is due to the production, by Drell-Yan, of τ lepton pairs having an invariant mass equivalent to m_{H^0}. In Table 2.2 we report the cross-sections and rates for different Higgs masses (20, 50, and 70 GeV) at $\sqrt{s} = 2$ TeV. Two cases are considered: 1 pb^{-1} per year and 0.05 pb^{-1} per year. These cases correspond to the luminosities expected after the first year and after the 1992 upgrade. We note immediately that there is no hope to find the H^0 in the first year(s) even if the mass is quite low. Provided with high luminosity (5×10^{31}cm^{-2}s^{-1}), the search for a low mass Higgs is feasible. The events as presented in Fig 2-1 are quite encouraging, with clear jet topologies. The ratio of signal to background is estimated to be roughly 1/20, which is not that large when compared with what is usually obtained at $p\bar{p}$ colliders. A sophisticated analysis taking advantage of the peculiar properties of the angular distribution of the τ's produced by the H^0 should provide a good way to overcome the background. Also it is important to note that such an upgraded Tevatron would, for the first time before LEP 200, be able to scan the mass range above 40 GeV up to 70-80 GeV; therefore it could have a good chance to discover the H^0 if its mass is in this region.

TABLE 2.2

Production of low-mass Higgs' at the $p\bar{p}$ Tevatron Collider ($\sqrt{s}$=2 TeV); estimates of cross-sections and rates (corresponding to an integrated luminosity L for 1 year of running of 10^{37} or 5×10^{38} cm^{-2}).

Process	m_{H^0} (GeV)	σ^* (pb)	Rates (events/year) L=10^{37}	L=5×10^{38}
$p\bar{p} \to H^0 \to \tau^+\tau^-$	20	5.5	12	600
$p\bar{p} \to H^0 \to \tau^+\tau^-$	50	0.3	-	35
$p\bar{p} \to H^0 \to \tau^+\tau^-$	70	0.16	-	20

* The cross-sections quoted in this Table are computed using the Pythia M.C. and include the branching ratios of $H^0 \to \tau^+\tau^-$. The rates include, in addition, the branching ratio of each τ into $\pi^{\pm}(n\pi^0)\nu_\tau$.

Now let us go ahead and consider a pp collider of $\sqrt{s} = 10$ TeV and 10^{39}cm^{-2} integrated luminosity per year or an 18 TeV pp machine with 10^{39} and 10^{40} cm^{-2} integrated luminosity. These would correspond to the LHC project.[9] In this case, we obtained for Higgs bosons with 50 or 100 GeV masses, the expected rates quoted in Table 2.3 (which includes branching ratios for $H^0 \to \tau^+\tau^-$ and each τ decaying into $\pi\nu_\tau\pi^{0\prime}s$). Again, a crude estimate of the corresponding background gives a signal over background of 1/20 to 1/30 which we should be able to deal with. The rates we obtained are quite reasonable for the two quoted masses. Pictures of events generated with the Pythia Monte Carlo and simulated in the CDF detector are presented in Fig 2.2. The pictures as well as the performance of CDF on these events is encouraging.

TABLE 2.3

Rates, cross-sections and backgrounds for the production of low mass Higgs' at 10 TeV and 18 TeV pp collisions for the process: $pp \rightarrow H^0 \rightarrow \tau^+\tau^-$ (calculated using the Pythia M.C.).

$\sqrt{s}$ (TeV)	H^0 Mass (GeV)	σ^* (pb)	Rate** (year^{-1})	S/B
10	50	3.0(4.3)	75(100)	.1(.1)
10	100	.15(.95)	4(25)	.005(.033)
18	100	.36(2.4)	80(550)	

* The numbers outside of brackets were calculated using a 40 Gev top mass and EHLQ structure functions;the numbers inside of brackets were calculated using a 100 GeV top mass and Wu-Ki-Tung structure functions.

** The rates correspond to an integrated luminosity of 10^{39} cm^{-2} per year and include the $\tau^{\pm} \rightarrow \pi^{\pm}(n\pi^0)\nu_\tau$ branching ratio.

In conclusion, it is quite clear that very low mass Higgs ($m_{H^0} < 30\ GeV$) will certainly be observed by presently designed e^+e^- colliders; LEP 200 would be a very good machine to scan the zone below the W mass (40 to 80 GeV). However, the Tevatron at high luminosity will certainly be able to look for Higgs in this mass range, maybe even before LEP200 (provided the upgrade in luminosity is achieved within the foreseen schedule).

2.2 Search for Intermediate Mass Higgs

If the Higgs mass is around $2m_W$ then the way to proceed becomes touchy. It seems, according to the present studies, that it would be too high a mass region for an e^+e^- collider such as LEP200. On the contrary, it is too low a mass range for an SSC machine (see Table 2.4). So let's try to compare the capabilities of the three types of colliders, e^+e^-, ep and pp, to search for a Higgs with a mass around 300 or 400 GeV. To do so, we have plotted the cross-section to produce Higgs' with masses of 300 GeV (solid line) and 400 GeV (dashed line) as a function of $\sqrt{s}$ in TeV for the three colliders, Fig 2.3. They each assume an integrated luminosity of 10^{32}cm^{-2}s^{-1} (i.e. 10^3 pb^{-1}/year). We may try to compare these results. The ideal would be to obtain for each of them an estimate of the number of events that would finally remain (real "H^0 candidate sample") once all the filters needed to extract the signal from the background have been applied. Such a detailed study has so far not been done for all three cases. What we may derive out of these three curves, as first information, is the $\sqrt{s}$ necessary to produce a certain number of Higgs bosons (say 100 per year) with a given mass and a given integrated luminosity. We see that at $\sqrt{s}_{e^+e^-} = 1$ TeV, we get 100 H^0's per year at a mass of 300 GeV. To get the same number of H^0's produced at an ep collider with the same mass and the same luminosity, we would need $\sqrt{s}_{ep} =$ 2.2 TeV. To obtain the same results in the case of a pp collider it would require $\sqrt{s}_{pp}$ = 6.2 TeV. As we will see when discussing the backgrounds in the various machines, while e^+e^- and ep colliders may be compared to a certain extent (at least in this type of scenario as the backgrounds are more or less of the same type and same order), it is quite clear that this is not the case with pp colliders where the type of backgrounds is drastically different and their amount relative to the signal is much greater. This implies that in the case of a pp collider it will be good to work with an higher c.m.

energy (compared to 6.2 TeV) in order to get one or two more orders of magnitude higher rate of events. Then, harder cuts can be applied to reduce the background and still obtain a comparable number of H^0's in the final sample of candidate events. Therefore we will compare here a 1 TeV e^+e^- machine with a 2 or 2.5 TeV ep machine and a 10 or 18 TeV pp collider (with the same luminosity or 10 times more).

TABLE 2.4

Higgs-Mass Discovery Limit as a function of $\sqrt{s}$ in $pp \rightarrow H^0 \rightarrow WW$ (see reference 10).

$\int Ldt$ (cm^{-2})	$\sqrt{s}$ (TeV)	m_{H^0} discovery limit (GeV)
10^{38}	20	–
	40	200
10^{39}	20	250
	40	400
10^{40}	20	700
	40	1000

We know that the technique to build a 1 TeV e^+e^- collider is not yet available. Two solutions for a super ep collider are foreseen; an ep collider in the LEP tunnel would have $\sqrt{s}$ of the order of 1.4 to 1.85 TeV and a luminosity of $10^{32}cm^{-2}s^{-1}$; an ep-SSC collider would have $\sqrt{s}$ = 1 to 4 TeV c.m. energy and the same luminosity as the ep-LEP project.Therefore we are going to study the performances of such super-ep machines for the search of intermediate mass Higgs bosons and compare them with a pp collider of 10 or 18 TeV c.m. energy.

2.2.1 Intermediate Mass Higgs and Very High Energy *ep* Colliders

A study has been pursued to emphasize the possibilities of ep machines to search for Higgs. The case of HERA and low mass Higgs is as pessimistic as the case of the Tevatron with low luminosity. If we consider an ep machine with electron beam energy between 75-100 GeV (which is at the limit imposed by synchrotron radiation) and a proton beam of 20 TeV, we will have $\sqrt{s} = 2.4 \rightarrow 2.8$ TeV. At these energies, a H^0 with $2m_W$ is mainly produced by WW or Z^0Z^0 fusion. The corresponding cross-sections for Higgs bosons with masses of 100, 200, and 300 GeV are listed in Table 2.5. As in the case for pp collisions, we may consider the effective mass approximation calculation and the exact calculation. Both numbers are quoted in this table. In the case of WW fusion, the ratio of $\sigma_{\text{approx}}/\sigma_{\text{exact}}$ is of order 1 to 2, in the case of Z^0Z^0 fusion, it is closer to 2-3.

TABLE 2.5

Cross-Sections in pb for the processes: ep $\rightarrow$ $H^0(WW)\nu$ X and ep$\rightarrow$ $H^0(ZZ)$eX for different values of $\sqrt{s}$ and H^0 mass. The first line gives the exact calculation with the second being the approximate.

	ep $\rightarrow$ WWν X			ep $\rightarrow$ ZZeX		
m_{H^0}	100	200	300	100	200	300
$\sqrt{s}$ (TeV)						
1.00	0.23	0.04	0.01	0.06	0.01	0.02
	0.09	0.02	0.01	0.02	0.01	.001
2.43	0.96	0.34	0.15	0.29	0.09	0.04
	0.49	0.21	0.10	0.10	0.05	0.02
2.83	1.15	0.43	0.21	0.35	0.12	0.06
	0.60	0.27	0.15	0.12	0.06	0.03

The main differences between ep and pp colliders are coming from the backgrounds. If m_{H^0} is larger than $2m_W$, the main Higgs production mechanism in ep collisions goes through the WW fusion and then the produced H^0 decays into 2 W's. Moreover, the question of backgrounds is much more favorable for ep machine than pp machines for the following reasons. First, in ep machines, there is not a QCD type background; i.e. pp $\rightarrow$ qq or qg with a radiated W by one of the partons. The only W radiation effect that one may have is through electroweak interactions such as :

$$eq \rightarrow \gamma, Z^0 \rightarrow \nu + q + W$$

$$eq \rightarrow \gamma, Z^0 \rightarrow e + q + W$$

and

$$eq \rightarrow W \rightarrow \nu + q + W$$

$$eq \rightarrow W \rightarrow e + q + W$$

where the W is radiated by the final leptons (neutrino or e) or the final parton (q or g). This type of background is very very small and can hardly simulate a W-pair. Similarily, in ep collisions there is the (W+jet(s)) background of the pp collisions but once again, as they are electroweak interactions, they are indeed very small (which is not the case as we have seen for pp collisions). Also, in ep interactions there are no backgrounds of the type WW continuum as we have in pp or e+e-:

$$e^+e^- \rightarrow W^+W^- \text{ or } pp \rightarrow W^+W^-$$

The only serious background is due to the processes in Figure 2.4 that we call respectively WW-background and $\gamma\gamma$-background; they both give a W-pair signal which will mimic the H^0.

In the case of an ep collider, the Higgs signal will be a "bump" in the invariant mass distribution of the process $ep \rightarrow WW$ over the continuum background. This is similar to the case of an e^+e^- machine; but, as we will see in Section 5, quite different from

the H^0 signal in pp machines where one has to "dig very hard" in order to extract the real signal from the "standard mess".

We have plotted in Figure 2.5 and 2.6 the invariant mass distributions, $d\sigma/dM_{WW}$, for Higgs masses of 200, 300 and 400 GeV at $\sqrt{s}$ of the 1 TeV and 3 TeV. We have separated the contributions coming from the process (a):$e^-q \to e^-WWX$ produced via WW fusion (solid line) from the ones due to the process (b):$e^-q \to e^-WWX$ produced through $\gamma\gamma$ fusion (dashed line). In the neigborhood of the resonance, almost all the contribution of process (a) comes from the s-Higgs-channel, and a clear bump appears in each mass case above the contribution of the $\gamma\gamma$ background. These results are slightly overestimated, as they have been obtained using the WW effective approximation; but, in particular at the Higgs resonance, this approximation works well and gives a realistic size of the peak.

This study shows, as an interesting result, that an optimal window for the search for Higgs bosons with an intermediate mass, say between 200 to 400 GeV, is obtained with this kind of super ep-collider.

2.2.2 Intermediate Mass Higgs and Intermediate Energy *pp* Colliders

A further study of a 10-18 TeV pp collider was made to get a better idea of the problems of detecting a Higgs at around 200 GeV.

The cross-sections and rates have been computed using the Pythia Monte Carlo assuming 2 cases. In one case the t-quark has the cannonical mass of 40 GeV and EHLQ[10] structure functions are used. In the second case, we assume a t-quark mass of 100 GeV and structure functions as calculated by Wu-Ki-Tung.[11] Both sets of numbers are quoted in Table 2.6. In this table we list separately each elementary process to show what fusion mechanism is predominant in each case. In particular, gg fusion is larger than $q\bar{q}$ fusion by a factor of about five. It is larger than ZZ and WW mechanisms by a factor of about two. The events at $\sqrt{s} = 10$ TeV have also been generated by Pythia for $m_H = 200\ GeV$ and have been fully simulated in the CDF detector in its present size and configuration. Such events are fully contained in such an apparatus even with 10 TeV collisions. Typical events can be seen in Figure 2.7. Despite the huge QCD background, it may be possible to detect these events as we will show in section 5. The rates are quite significant. Therefore, looking for intermediate mass Higgs with such pp colliders should be equivalent to looking for higher mass Higgs at the SSC.

It seems improbable that a very high energy e^+e^- collider ($\sqrt{s} = 300 \to 400\ GeV$) will be built by 1995. There is room both for a high energy ep ($\sqrt{s}$ between 2 and 3 TeV) and a pp collider with $\sqrt{s} = 10 \to 18$ TeV with $10^{32-33}\text{cm}^{-2}\text{s}^{-1}$ luminosity to scan the intermediate mass region near 200 GeV. In addition, this is a very interesting region as the WW fusion mechanism starts to take effect.

TABLE 2.6

Rates, cross-sections and backgrounds for the production of intermediate (200 GeV) mass Higgs' in 10 TeV and 18 TeV pp collisions for the process $pp \rightarrow H^0 \rightarrow W^+W^-$ where $W \rightarrow e\nu$ and $W \rightarrow q\bar{q}$ (calculated using the Pythia M.C.).

$\sqrt{s}$ (TeV)	Process	σ * (pb)	Rate** ($year^{-1}$)	Background Processes	Background σ (pb)
	$q\bar{q} \rightarrow H^0 \rightarrow WW$	1.7(1.6)		W + jet ($p_t^{q,g} > 100GeV/c$)	3100
18	$gg \rightarrow H^0 \rightarrow WW$	7.2(18)	12000 (24000)	W + jet ($p_t^W > 100GeV/c$)	420
	$WW + ZZ \rightarrow H^0 \rightarrow WW$	3.0(4.2)		WW continuum WZ continuum ($p_t^{W,Z^0} > 100GeV/c$)	7 .43
	$q\bar{q} \rightarrow H^0 \rightarrow WW$	.57(.48)		$qg \rightarrow qg + W_{rad}$ ($p_t^{q,g} > 100GeV/c$)	1000
10	$gg \rightarrow H^0 \rightarrow WW$	2.4(4.9)	400(770)	W + jet ($p_t^W > 100GeV/c$)	160
	$WW + ZZ \rightarrow H^0 \rightarrow WW$	1.1(1.3)		WW continuum WZ continuum ($p_t^{W,Z^0} > 100GeV/c$)	3.3 0.2

*The numbers outside the brackets were calculated using a 40 GeV top mass and EHLQ structure functions; the numbers inside the brackets were calculated using a 100 GeV top mass and Wu-Ki-Tung structure functions.

**The rates correspond to an integrated luminosity of $10^{38}(10^{39})$ cm^{-2} per year and are the sum of all channels. In this case no branching ratios have been included in the rates. If one W decays leptonically and the other hadronically, then the quoted numbers should be divided by 10.

2.3 High Mass Higgs and Very High Energy pp Colliders (SSC)

If the Higgs has a mass from 300 GeV to 1 TeV, by taking into account our present knowlege of the techniques of acceleration, a very high energy pp collider such as the SSC is the only accelerator that will be able to scan this mass range.

Therefore, we define the main scenarios that will be considered and discussed in the following sections. At the UCLA[12] meeting, it was decided to concentrate effort on the two main processes:

$$pp \rightarrow H^0 \rightarrow WW \tag{2.2}$$

where one W decays leptonically and the second hadronically and

$$pp \rightarrow H^0 \rightarrow Z^0Z^0 \tag{2.3}$$

where one Z^0 decays into $\nu\bar{\nu}$ and the other Z^0 decays into a pair of leptons (e or μ). The case where both Z^0's decay into leptons (4 leptons) is also taken into account and considered as a set of rare "gold plated" events.

We also will briefly discuss the case of a charged Higgs because the standard model does not prohibit processes like:

$$t\bar{b} \rightarrow H^{\pm} \rightarrow \tau^{\pm}\nu_{\tau}$$

This process is considered for a non-minimal Higgs with a mass of 300 GeV[13].

For the "standard Higgs", two masses are considered (300 and 800 GeV). The main backgrounds which compete with process 2.2 and 2.3 are by increasing order of importance:

$$pp \rightarrow WZ^0$$

$$pp \rightarrow W^+W^- \text{or} Z^0Z^0$$

$$pp \rightarrow W \text{ jet or } Z^0 \text{ jet}$$

$$pp \rightarrow q, g + W_{\text{radiated}}$$

where the W in the last equation is radiated by one of the final partons.

In conclusion, it is quite clear that a low mass Higgs ($m_H \leq 40\ GeV$) will be accessible by the present generation of e^+e^- colliders. LEP 200 and the Tevatron (with high luminosity) will be able to scan the mass range from 40 to 70 GeV. If present schedules are adhered to, the Tevatron should see the first events followed by LEP 200 which will be operating mainly within this favored mass range. An intermediate Higgs with $m_H \approx 200\ GeV$ would favor an ep collider with $\sqrt{s} \approx 2 - 3\ TeV$ or a 10-18 TeV pp collider such as LHC, unless it becomes feasible to build a $\geq$400 GeV e^+e^- collider. To access the puzzling 1 TeV range, it is quite clear that a pp collider such as the SSC is the best gadget in a reasonable time scale. We summarize the different alternatives in Figure 2.8.

3. Rates for Signals and Backgrounds

In this section, we summarize the expected rates for each of the high mass Higgs scenarios defined in Section 2. A nominal luminosity of $10^{33}\text{cm}^{-2}\text{s}^{-1}$ (10^{40}cm^{-2} per year) is assumed. These rates and cross sections have been computed using the Pythia Monte Carlo. They have been cross-checked with the theoretical expectations after taking into account the imposed cuts. The quoted numbers already include the branching ratios of the decays, as well as the cuts on the mass of the Higgs or on the p_t range of the decay products. No cut on the rapidity range has been applied. These imposed conditions are explicitely mentioned in the corresponding Tables (3.1, 3.2 and 3.3).

In Table 3.1, we list the cross-sections and rates corresponding to the signal: $pp \rightarrow H^0 \rightarrow WW$, where one W decays leptonically and the other one hadronically; the H^0 is assumed to have a mass of 300 GeV or 800 GeV. Also in this table are quoted backgrounds due to:

- the W-pair continuum, where the W's decay like W's from H^0 decay and have transverse momentum: $p_{tW} \geq 150\ GeV$ (to be equivalent to a H^0 mass around 300 GeV) or $p_{tW} \geq 350\ GeV$ (to be equivalent to a H^0 mass around 800 GeV).
- the WZ^0 continuum, with the same constraints on p_t of the W and Z^0 as above and where the W decays leptonically and the Z^0 hadronically.
- the W + jet signal, where both the W and the recoil jet are required to have a transverse momentum compatible with the masses of the H^0, and where the W decays leptonically.

- the QCD background, where one of the partons radiates a W, with the same cut on the transverse momentum of the partons as for the previous case. The radiated W is forced to decay leptonically to $e\nu$.

We note that the case where the H^0 decays into W-pairs provides a relatively large number of events, compared to the Z^0-pair decay, by about a factor of 25. Continuum WW or WZ production provides a signal to background (S/B) of order 1, in both cases; whereas, the dominant backgrounds are from W + jet and QCD jets with a radiated W. The ratio S/B is about 3×10^{-3} for the W + jet background and even a factor of 10 higher for the QCD background; these values of S/B for the standard background correspond to the case of a relatively low mass Higgs ($m_{H^0} \approx 300\ GeV$). The high mass Higgs ($m_H \approx 1\ TeV$) has much smaller backgrounds. The value S/B for W + jet becomes about 10^{-2} whereas for the (QCD+radiated W) background it is of order 5×10^{-3}, about a factor of 10 lower than for a 300 GeV H^0. This gives an indication, which will be confirmed later, that the 800 GeV case is easier than the 300 GeV case at the SSC.

TABLE 3.1

Signal/Background rates for $pp \rightarrow H^0 \rightarrow WW$ for an integrated luminosity of $10^{40}\mathrm{cm}^{-2}\mathrm{s}^{-1}$ (calculated using the Pythia M.C.).

Process	Sigma (mb)	Rate/year (number of events)
$H^0 \rightarrow WW$ with W $\rightarrow e\nu$ or $\mu\nu$ and $W \rightarrow q\bar{q}$		
$m_{H^0} = 300$	4.3×10^{-9}	43000
$m_{H^0} = 800$	3.6×10^{-10}	3600
$pp \rightarrow WW$ with W $\rightarrow e\nu$ or $\mu\nu$ and $W \rightarrow q\bar{q}$		
$p_{tW} > 100$	4.1×10^{-9}	41000
$p_{tW} > 350$	1.1×10^{-10}	1100
$pp \rightarrow WZ$ with W $\rightarrow e\nu$ or $\mu\nu$ and $Z \rightarrow q\bar{q}$		
$p_{t(\mathrm{W\ or\ Z})} > 100$	0.84×10^{-9}	8400
$p_{t(\mathrm{W\ or\ Z})} > 350$	2.3×10^{-11}	230
pp $\rightarrow$ W + jet with W $\rightarrow e\nu$ or $\mu\nu$		
$p_{tW} > 100$	1.44×10^{-6}	1.4×10^{7}
$p_{tW} > 350$	2.8×10^{-8}	0.28×10^{6}
pp $\rightarrow$ qq, qg, gg with one parton radiating a W; factor 10^{-3}		
$p_{t(\mathrm{q\ or\ g})} > 100$	$1.3 \times 10^{-2} \times 10^{-3}$	1.3×10^{8}
$p_{t(\mathrm{q\ or\ g})} > 350$	$8.6 \times 10^{-5} \times 10^{-3}$	8.6×10^{5}

In Table 3.2, we list the cross-sections and rates which correspond to the signal: $pp \rightarrow H^0 \rightarrow Z^0Z^0$ where one Z^0 decays into 2 charged leptons (e or μ) and the other Z^0 decays into $\nu\bar{\nu}$ (where $\nu = \nu_e$, ν_μ, or ν_τ) for the two cases ($m_H = 300\ GeV$ and $800\ GeV$). The background due to Z^0Z^0 or Z^0W continuum which may mimic the H^0 signal is also listed. The Z^0W continuum where the W decays into $e\nu$ and Z^0 into $\nu\bar{\nu}$ takes into account the case where one lepton is lost. Another possibility to mimic the Higgs signal is given by the Z^0W continuum when the Z decays into a pair of charged leptons and the W decays hadronically. This background signature is very

similar to that provided by the sample of (Z^0 + jet) events; again the missing energy will be generated by the mismeasurement and/or the semileptonic decay of the hadrons produced by the decay of the W. The continuum background gives a S/B of order 1. The background from (Z^0 + jet) gives a S/B ratio which varies from 10^{-3} for the 300 GeV case to 5×10^{-3} for the 800 GeV case. If we consider the case of $H^0 \rightarrow Z^0Z^0$ where both Z^0's decay leptonically (e or μ), we obtain from the Pythia Monte Carlo an estimated cross-section of 3×10^{-11} mb for a 300 GeV H^0 and 2×10^{-12} mb for an 800 GeV H^0. To have a correct estimate of the rate of expected events, we must fold in the multi-lepton recognition efficiency. This will be done in section 5.

TABLE 3.2

Signal/Background rates for $pp \rightarrow H^0 \rightarrow ZZ$ for an integrated luminosity of $10^{40}\text{cm}^{-2}\text{s}^{-1}$ (calculated with the Pythia M.C.).

Process	Sigma (mb)	Rate/year (number of events)
$H^0 \rightarrow ZZ$ with Z $\rightarrow$ ee or $\mu\mu$ and $Z \rightarrow \nu\bar{\nu}$		
$m_{H^0} = 300$	1.7×10^{-10}	1700
$m_{H^0} = 800$	1.7×10^{-11}	171
$pp \rightarrow ZZ$ with Z $\rightarrow$ ee or $\mu\mu$ and $Z \rightarrow \nu\bar{\nu}$		
$p_{tZ} > 100$	8.3×10^{-11}	830
$p_{tZ} > 350$	2.6×10^{-12}	26
$pp \rightarrow WZ$ with $W \rightarrow e\nu$ and $Z \rightarrow \nu\bar{\nu}$		
$p_{t(\text{W or Z})} > 100$	1.1×10^{-10}	1100
$p_{t(\text{W or Z})} > 350$	3.2×10^{-12}	32
pp $\rightarrow$ Z + jet with Z $\rightarrow$ ee or $\mu\mu$		
$p_{tZ} > 100$	1.9×10^{-7}	1.9×10^{6}
$p_{tZ} > 350$	3.6×10^{-9}	36000
$pp \rightarrow b\bar{b} + t\bar{t}$		
$p_{t(\text{b or t})} > 100$	1.2×10^{-4}	1.2×10^{9}
$p_{t(\text{b or t})} > 350$	7.5×10^{-7}	7.5×10^{5}

In Table 3.3, we emphasize the case of a 300 GeV charged Higgs and its background: $W \rightarrow \nu\tau$. As mentioned in Section 2, most work has concentrated on the minimal neutral Higgs and its decays into IVB-pairs. However, the charged Higgs is possible in the standard model and is favored in some scenarios beyond the standard model. Moreover, the signature we emphasize is quite attractive for the experimentalist because the τ-signal is one of the major tools of pp physics, as evidenced at low energy.[14] From Table 3.3 the S/B ratio is 5×10^{-3}; we will see in section 5 how to overcome it.

The main conclusions from these estimates is that the signals give decent rates at the SSC; however, very high standard backgrounds must be overcome. Most of what follows will show how to we try to achieve this goal; in particular, we will compare the W-pair versus the Z-pair cases and the purely leptonic signatures versus the mixed leptonic and hadronic signatures.

TABLE 3.3

Signal/background for $t\bar{b} \rightarrow H^{\pm} \rightarrow \tau\nu_{\tau}$ (calculated with the Pythia M.C.).

$\sigma(H^{\pm} \rightarrow \tau\nu_{\tau})$	$= 1.8 \times 10^{-11}$ mb (if top=40GeV and EHLQ's structure function)
	$= 3.1 \times 10^{-11}$ mb (if top=40 GeV and Wu Ki Tungs structure function)
$\sigma(W^{\pm} \rightarrow \tau\nu_{\tau})$	$= 4.8 \times 10^{-9}$ mb for $p_{tW} > 300$ Gev
	$= 7.7 \times 10^{-9}$ mb for $p_{tW} > 250$ GeV

Remark: Both numbers are not very different if one varies the top mass to 120 Gev or 200 Gev.

4. Main Characteristics of the Events; Trigger Strategy

To analyze the characteristics of the events of interest: W- and Z-pairs, H^o events, and their associated backgrounds, we had to first construct a Monte Carlo generator. At the time we started this work, January 1986, we had at our disposal two general purpose programs designed to study pp interactions: Isajet[15] and Pythia[7]. Neither of them had been implemented with all the necessary processes. Therefore, an important first step has been to build and test the appropriate generator routines. It was necessary to insert Higgs production, via all possible mechanisms: $q\bar{q}$, gg, WW or ZZ fusion, and hadroproduction as well as the QCD background represented by the 2 to 3 process:

$$qg \rightarrow qg + W_{\text{radiated}}$$

(this is mimicked in the Monte Carlo using pp $\rightarrow$ W+q or g where the final parton emits a gluon by gluon bremstrhalung and applying an appropriate set of cuts). Also a fair amount of work has been done to correctly reproduce the soft gluon contribution.[16] Once the reactions were introduced, the results obtained by each Monte Carlo were compared to each other and to the theoretical predictions. Most of this work was done before the Snowmass '86 meeting and the results are contained in reports from the UCLA[12] and Madison[17] workshops. As of now, only Pythia has the Higgs production fully implemented.

4.1 Generation of Higgs by Pythia

For a complete and detailed explanation of Pythia, we refer the reader to the contribution of Bengsston and Sjöstrand in these Proceedings.[18] Here we describe how the Higgs and W-pair events have been generated for the studies reported in this paper.

The signals and backgrounds for Higgs production in this work have been generated using the Lund Monte Carlo for Hadronic Processes, Pythia[18]. The program includes the four standard channels for Higgs production, *viz.* $q\bar{q} \rightarrow H^0$, $gg \rightarrow H^0$, $Z^0Z^0 \rightarrow H^0$, and $W^+W^- \rightarrow H^0$. The cross-sections for these processes are all taken from ref. 10, but the zero width approximation for the Higgs is replaced by the normal Breit-Wigner shape; the width of the Higgs is calculated to first order in the coupling constant. For the last two channels, i.e. vector boson fusion to Higgs, the absolute cross-section is calculated in the effective W-(Z-)approximation, but p_t etc. are generated according to the correct matrix element, as given e.g. in ref. 19. The normalization of vector

boson fusion could thus be off by a factor two or so; also, as has been pointed out by Gunion et al.,[20] the cross-section for $q\bar{q} \rightarrow H^0$ is an overestimate when m_t is not much smaller than m_H. Decay of the Higgs is performed taking the proper matrix element into account, so that correct angular distributions are obtained for the decay chain $H^0 \rightarrow Z^0Z^0, W^+W^- \rightarrow 4$ fermions. In addition to the standard model neutral Higgs, Pythia also includes the option of generating a charged Higgs, $H^{\pm}$.[20]

The backgrounds to the different Higgs signals come from processes like $q\bar{q} \rightarrow Z^0Z^0$, $q\bar{q} \rightarrow W^+W^-$, $q\bar{q}' \rightarrow Z^0W^{\pm}$, $q\bar{q}' \rightarrow W^{\pm} + 2$ jets, etc. All processes of the type $2 \rightarrow 2$ have been included in Pythia (see ref. 18); for processes like $q\bar{q}' \rightarrow W^{\pm} + 2$ jets, which are properly of the type $2 \rightarrow 3$, generation is accomplished by using a $2 \rightarrow 2$ subprocess like $q\bar{q}' \rightarrow W^{\pm} + g$ and selecting those events where initial state radiation creates a second jet of sufficient energy and transverse momentum to pass the cuts. For most of phase space, this should be rather a good approximation to the exact result.

Absolute cross-sections will depend on the structure functions used; Pythia includes the revised EHLQ sets,[10], as well as the parametrizations of Duke and Owens,[21] and Glück, Hoffman and Reya.[22] In addititon to these parametrizations, Pythia can also be run together with the structure function evolution program of Wu-Ki Tung;[11] the differences in absolute cross-sections are especially noticeable for processes involving heavy quarks, where the scheme of Wu-Ki Tung gives substantially higher values.

4.2 Main Properties of Generated Higgs Events

The next step in this study was to look at the main properties of the Higgs events generated by Pythia. This is done both to verify that the Monte Carlo agrees with theoretical expectations and also as a guide for the event analysis.

For the process $H^o \rightarrow WW$, we have looked at two properties. The first one is the angle between the two W's, $\Delta\phi_{WW}$. We show in Figure 4.1 the distribution of this parameter as well as its change as the Higgs mass is varied from 300 to 800 GeV; this distribution is much sharper for higher mass Higgs'. If we require $\Delta\phi$ to be less than 150°, we note that 57.7% of 300 GeV Higgs' pass this cut as opposed to 17% of the 800 GeV sample. If we now require that $\Delta\phi < 120°$, 33% (4.5%) of the 300 (800) GeV events pass this condition. Another important characteristic is the angle between the two jets coming from the decay of one of the W's. We see that, as expected, the angle decreases as the Higgs mass increases (Fig. 4.2). For example, the average value of this quantity is 36.5° when the Higgs mass is 300 GeV and is only 10.4° for 800 GeV masses.

A display program, interfaced directly to the generator package, has been written which allows visualization of the generated events. Displays of the original parton momenta, reconstructed jet momenta, final particle momenta, and tracks in a detector with and without magnetic field were generated. These pictorial views of events provide a great deal of physical intuition about the topology of large multiplicity, high energy events and show the limitations of naive jet reconstruction. This insight is very suggestive about what constitutes a sensible detector.

The following type of events are displayed here: low p_t QCD events (minimum bias events) with $p_t < 10$ GeV (Fig 4.3), high p_t QCD events with $p_t = 1$ TeV (Fig 4.4), $H^0 \rightarrow WW$ signal with m_{H^0}=300 GeV (Fig 4.5) or m_{H^0}=800 GeV (Fig 4.6), where one of the W's decays leptonically and the other one hadronically and finally $H^0 \rightarrow Z^0Z^0$ with m_{H^0}=300 GeV (Fig 4.7) or m_{H^0}=800 GeV (Fig 4.8) and where one Z^0 decays into 2 charged leptons and the other decays into $\nu\bar{\nu}$.

In conclusion, analysis of the generated events tells us that the signal $H^o \rightarrow WW$

with $m_{H^0} \approx 300$ GeV will be more difficult to identify than at higher masses. This is due primarily to the fact that the W's are less "back-to-back" at the lower masses. Also, the two jet decay products of the W have larger separations for low-mass Higgs' which will complicate the recognition due to the presence of "spectator-jets". For high mass events the two-jet system is much more collimated. Finally, the W's from a relatively low mass Higgs are much more likely to lie in the very forward direction as they are produced with lower p_t.

4.3 Ideal Detector Analysis:Main Properties of the Events

We begin our event analysis using a simple program which simulates an idealized 4π fine-grained calorimeter containing both an e.m. and hadronic sections but no cracks or dead regions. The energy of each particle is completely confined to single towers but shared between e.m. and hadronic layers. Energy "smearing" is introduced to simulate calorimeter resolution. This simulation package was developed at Snowmass '84[24]. It also contains a simple jet algorithm used to analyze the clusters in the event.

The analysis of WW events begins by first trying to reconstruct the W which decays leptonically. It takes the highest p_t electron with the requirement that the transverse momentum be greater than 20 GeV (electrons are 100% "identified" using the Monte Carlo particle information. It then requires that the total transverse missing energy, E_t^{miss}, measured by the calorimeter be larger than 20 GeV. It compares E_t^{miss} to the p_t of the highest ν in the event and to the sum over all ν's ($E_t^{\nu's}$) (both given by the Monte Carlo). We have verified that E_t^{miss} and $E_t^{\nu's}$ are quite similar and not too different from the p_t of the highest ν. Next, the electron and E_t^{miss} are combined to calculate the transverse mass of the system. Quite a good agreement was obtained between this quantity and that of the initial $W \rightarrow e\nu$ system generated by the Monte Carlo. The only bias comes from not being able to measure the ν from the W decay but instead measuring the sum of all ν's in the event. We note that at least at this level of simulation both values are not dramatically different.

Once the first W (W_1) is reconstructed, the program attempts to reconstruct the second W which decays hadronically ($W \rightarrow q\bar{q}$). To do this, we work in the transverse plane compared to the beam axis and do the vectorial sum of the electron's and missing p_t's directions in this plane to obtain the W_1 observed direction. Then we define the "away" hemisphere by looking at the hemisphere which is defined by $\pm 90^\circ$ compared to the reconstructed W_1 direction. In the away hemisphere, the two highest E_t jets are used to reconstruct the second W. The results of this analysis for all the WW processes as given by Pythia and Isajet are summarized in Table 4.1.

TABLE 4.1a

Average values for the main characteristics of $H^0 \rightarrow WW$ events for a Higgs mass of 300 (800) GeV and its corresponding backgrounds.

Process	E_T^e (GeV)	E_T^{miss} (GeV)	Isol e (GeV)	M_T(e, miss) (GeV/c^2)	E_T^{jet1} (GeV)	E_T^{jet2} (GeV)
$H^0 \rightarrow W^+W^-$	75(189)	83(191)	4.7(4.8)	61(62)	130(340)	51(100)
WW continuum	75(206)	82(197)	4.7(6.7)	62(71)	136(405)	79(147)
WZ^0continuum ($Z^0 \rightarrow q\bar{q}$)	85(206)	73(191)	4.5(5.1)	68(77)	137(413)	77(143)
W + jet	70(188)	73(213)	4.8(7.4)	64(65)	139(398)	50(140)

TABLE 4.1b

Average values for the main characteristics of the WW continuum for a Higgs mass of 300 and 800 GeV and a comparison between Pythia and Isajet and between the observed average values as reconstructed from the analysis program and the true average values as directly given by the Monte Carlo (numbers in parentheses).

	ISAJET $100 \leq p_t^W \leq 200$	PYTHIA $100 \leq p_t^W \leq 200$	ISAJET $350 \leq p_t^W \leq 450$	PYTHIA $350 \leq p_t^W \leq 450$
E_T^e (GeV)	75(74)	60(63)	206(206)	205(220)
$E_T^{e^+}$ (GeV)	67(69)	60(68)	196(206)	223(238)
$E_T^{e^-}$ (GeV)	79(79)	58(60)	191(206)	174(198)
E_T^{miss} (GeV)	82(85)	88(86)	197(205)	180(194)
E_T^1 (GeV)	136(-)	131(-)	405(-)	399(-)
E_T^2 (GeV)	80(-)	79(-)	147(-)	126(-)
$m_T(e\nu)$ (GeV/c^2)	62(75)	60(75)	71(75)	89(75)
$m_T(j_1,j_2)$ (GeV/c^2)	194(-)	119(-)	411(-)	237(-)

The analysis of the Z^0Z^0 case follows almost the same lines. The first and second highest p_t electrons (e_1 and e_2) are each required to have p_t's greater than 20 GeV and are again identified as electrons with 100% efficiency. In addition, the highest e^+ and e^- (with the charge from the M.C.) are chosen. These are then compared to the electrons from the Z^0 decay and it was verified that looking for the two highest p_t electrons is a very efficient way to identify Z^0's. An away hemisphere is then defined with respect to the two electrons in the same way as for the WW case. The analysis then attempts to reconstruct the second Z^0 which decays into $\nu\bar{\nu}$. Using the calorimetry, E_t^{miss} in the away hemisphere is calculated and compared with the p_t of the two highest ν's (coming from the Z as given by the Monte Carlo). We find a very good agreement between E_t^{miss} and $E_t^{\nu's}$ which demonstrates the utility of this technique. Moreover, the program looks at the isolation of the electrons reconstructed in the event. Isolation is defined as the E_t in a cone of $\Delta R < .5$ (with $\Delta R = \sqrt{\Delta y^2 + \Delta\phi^2}$) minus the E_t

of the electron candidate. We list in Table 4.2 the main characteristics of the Z^0Z^0 processes.

TABLE 4.2a

Average values of the main characteristics of $H^0 \rightarrow Z^0Z^0$ events for a Higgs mass of 300 (800) GeV and its corresponding backgrounds. The $\Delta\phi$ refers to the azimuthal angle between the two electrons from the Z.

Process	$H^0 \rightarrow Z^0Z^0$	Z^0Z^0 continuum	WZ^0 continuum ($Z^0 \rightarrow \nu\bar{\nu}$)
E_T^{e1} (GeV)	93(229)	116(305)	80(177)
E_T^{e2} (GeV)	42(90)	57(105)	0(-)
$E_T^{e^+}$ (GeV)	63(169)	79(223)	76(167)
$E_T^{e^-}$ (GeV)	72(152)	98(204)	89(210)
Isol1 (GeV)	3.5(7.4)	1.4(3.2)	2.4(3.9)
Isol2 (GeV)	4.2(2.5)	1.7(4.7)	-(-)
E_T^{miss} (GeV)	117(275)	140(388)	106(217)
$E_T^{jet_1}$ (GeV)	133(171)	136(193)	111(196)
$E_T^{jet_2}$ (GeV)	102(89)	-(93)	70(102)
$m(e_1,e_2)$ (GeV/c^2)	88(96)	90(90)	-(-)
$\Delta\phi$ (deg)	15(35)	56(30)	-(-)

By looking at the results in Tables 4.1 and 4.2, we note that:

- A very good agreement is found between the observed and true quantities. This insures the efficacy of these analysis procedures.
- A very good agreement is found between the two Monte Carlo generators (Pythia and Isajet) for the same processes and conditions.
- The values in these table define trigger thresholds and allow, in some cases, to distinguish the signal from its major backgrounds.

These three points are now developed in a more detailed way.

For H^0 decays into W-pairs, the event characteristics are very similar to those of the backgrounds. Therefore, subtler procedures will be needed to enhance the real signal in this channel; this will be studied in detail in sections 5.2 and 5.3. Concerning the mean values of the most important quantities, the average E_t for either the electron or the missing energy is around 25% of the Higgs mass (e.g. 75 GeV for a 300 GeV Higgs). The average highest E_t jet is around 130 GeV and the second highest jet is between 50 and 75 GeV for low mass Higgs decays. For Higgs' of 800 GeV, the average value of these parameters become about 350 to 400 GeV for the highest E_t jet and 100 to 150 GeV for the second. These values will be of use when setting trigger thresholds (see section 4.4).

TABLE 4.2b

Average values of the main characteristics of the ZZ continuum for a Higgs mass of 300 and 800 GeV and a comparison between Pythia and Isajet and between the observed average values as reconstructed from the analysis program and the true average values as directly given by the Monte Carlo (numbers in parentheses). The $\Delta\phi$ refers to the azimuthal angle between the two electrons from the Z.

	ISAJET	PYTHIA	ISAJET	PYTHIA
	$100 < p_t^Z < 200$		$350 < p_t^Z < 450$	
$E_T^{e_1}$ (GeV)	111(111)	116(116)	296(296)	305(305)
$E_T^{e_2}$ (GeV)	50(44)	57(51)	113(107)	105(105)
$E_T^{e^+}$ (GeV)	83(77)	79(73)	171(165)	226(203)
$E_T^{e^-}$ (GeV)	82(78)	98(93)	245(238)	204(192)
Isol1 (GeV)	4.0(4.0)	1.4(1.4)	7.6(5.2)	3.2(3.2)
Isol2 (GeV)	5.0(3.4)	1.7(2.7)	7.5(4.3)	4.7(4.4)
$m(e_1,e_2)$ (GeV)	90(90)	90(90)	90(90)	90(90)
E_T^{miss} (GeV)	136(135)	140(142)	392(392)	388(390)
$\Delta\phi$ (deg)	65(72)	56(67)	24(29)	21(30)
$E_T^{jet_1}$ (GeV)	92(-)	136(-)	138(-)	193(-)
$E_T^{jet_2}$ (GeV)	63(-)	-(-)	86(-)	93(-)

For Z -pair events, the situation is quite different. While the Z^0Z^0 continuum and $H^0 \rightarrow Z^0Z^0$ events have very similar characteristics, those from the WZ^0 continuum (where $Z^0 \rightarrow \nu\bar{\nu}$ and $W \rightarrow e\nu$) will be easily suppressed by requiring two electrons above a given threshold. The only disturbing background in this case is the one due to $pp \rightarrow Z^0 +$ jet. The important criteria here is the rate passing a given missing energy cut. We show in figure 4.9 the E_t^{miss} distribution for the ZZ continuum where the transverse momentum of the Z is required to be above 150, 300 and 500 GeV (corresponding to Higgs masses of about 300, 600 and 1000 GeV). These events are characterized by a fair amount of missing energy. An analysis[12] has shown that, for (Z + jet) events with $p_t^{jet} > 500$ GeV, a cut on E_t^{miss} of 100 GeV gives a signal to background ratio (S/B) of 1 with a 200 GeV cut giving S/B of about 10. From this we conclude that a sufficiently high E_t^{miss} cut should sufficiently reduce the single (Z + jet) background while keeping a good fraction of the signal. Thus, though the Z-pair signals provide less rate then the W-pair signals (1/25), it will be much easier to extract this signal from its background by simple filter requirements at an early stage; namely requirements on 2 leptons and on E_t^{miss} at the first and second level triggers.

4.4 Trigger Strategy for W- and Z-pairs

The trigger is a main concern for the experimentalist at pp colliders (as opposed to e^+e^- machines). We can use what we summarized in Section 4.3 to set up a trigger strategy for W- and Z-pairs.

Preliminary studies[25] on W-pair triggering have already been done. The trigger scheme is sketched in Figure 4.10 and proceeds by defining a first level trigger based on selecting an electron candidate and requiring a minimum amount of E_t^{miss}. This is done

to try and reconstruct the W which decays leptonically. The electron is defined as a minimum amount of transverse energy, E_t^{cell}, in a calorimeter cell ($E_t^{cell} > 25GeV$); in addition 80% of this energy must be electromagnetic. The missing transverse energy as measured by the calorimeter must be larger than 40 GeV. The second level trigger imposes an isolation cut on the electron; this means that the region around the electron candidate defined by a zone of ± 5 calorimeter cells (both in pseudorapidity and azimuth) contains less than 20% of the transverse energy of the electron candidate cell. It also requires that in the hemisphere opposite the electron and missing energy there is either one jet with $E_t > 80$ GeV or two jets each with $E_t > 40$ GeV. Finally, a third level trigger requires the matching of a track with tranverse momentum greater than 10 GeV with the candidate electromagnetic cell.

Such requirements lead to a trigger rate of about 1 Hz. Note that after the first cut, we still have a 30 kHz rate. Also, this trigger defines quite low thresholds and, in fact, will trigger on relatively low mass Higgs' ($m_{H^0} > 200$ GeV). Such a strategy will have to be used, at least during early SSC runs, as m_{H^0} will be expected to be between 200 GeV and 1 TeV.

A trigger strategy for Z^0 pairs is defined along the same lines. A first level trigger requires a missing transverse energy greater than 100 GeV and two electrons; with the electron candidates being defined in the same way as in the W case above except that the E_t^e cut is raised to 40 GeV. Next, the second level trigger refines the estimation on E_t^{miss} and on the applied cut and also requires that each electron candidate match a track with $p_t > 20$ GeV. This trigger reduces the rate to about 1 Hz or less.

The aim of these triggers is to **preserve** as much as possible the expected H^0 signal over as wide a mass range as possible and meanwhile to **keep** a certain amount of the WW, WZ and ZZ continuum. The continuum sample is an interesting sample both to study the properties of Higgs background and also to look for possible interesting physics[26].

These trigger strategies, based on an idealized 4π detector, show the feasibility of these searches and give some ideas on how to analyze the possible signals. The work is then refined in the next section using a more "realistic" simulation.

At this stage of our work, we have understood why it is worthwhile to pursue the search for the WW and Z^0Z^0 continuum as well as conventional Higgs' in a high energy pp collider environment. We have setup various scenarios to identify such events. We have estimated their rates as well as their main backgrounds and have shown the main characteristics of these signals as well as a strategy to extract them from the standard backgrounds in an ideal case (i.e. a 4π fine-grained calo- rimeter without any dead area). We know from this "simplified" point of view that it is possible to search for these signatures. Therefore it is justified to pursue this work along the lines we have defined but implementing now a more realistic reproduction of the enviroment which will have to be dealt with at the SSC. This is what we finally tried to achieve in this working group. For that, we refer the patient reader to the second report of our work located elsewhere in this Proceedings under the following title: "Detecting W/Z Pairs and Higgs' at High Energy Colliders:Main Experimental Issues."

References

[1] G. Arnisson et al., UA1 Coll., Phys.Lett. **122B**, 103 (1983); M. Banner et al., UA2 Coll., Phys.Lett. **122B**, 476 (1983); G. Arnisson et al., UA1 Coll., Phys.Lett. **126B**, 398 (1983); P. Bagnaia et al., UA2 Coll., Phys.Lett. **129B**, 130 (1983).

[2] See the presentations of results from both the UA1 and UA2 Collaborations at the 6th Topical Workshop on Proton-Antiproton Collider Physics at Aachen (July 1986) and at the Int. Conf. on High-Energy Physics, Berkeley, Cal., 1986.

[3] For a description of the possibilities of a LEP200 machine see for instance: G. Barbiellini et al., "Physics at LEP at high energies" in "Physics at LEP", CERN 86-02 Vol.2 (1986); P. Bernard, H. Lengeler and E. Picasso, LEP note 524 CERN/EF/RF 85-1.

[4] The results reported in the Subsection 2-2-1 and the Table 2-1 are directly derived from the transparencies of the talk given at the ECFA Workshop "LEP200", Aachen, (Sept. 29-Oct. 1, 1986), by S. L. Wu on the "Search for Higgs at LEP200." Therefore these conclusions are preliminary and one should refer to the written version of this talk to appear in the Proceedings of this Workshop for definite numbers.

[5] The study on low mass Higgs' at pp colliders has been initiated at the Madison Workshop (May 1986) by H.-U. Bengtsson, A. Savoy-Navarro and Y. Takaiwa, also see the report of A.S.N. to appear in these proceedings (Ref 17).

[6] B. Cox, F.J. Gilman, "Report of the working group on Standard electroweak interactions and Higgs", Snowmass'84 Proceedings page 87. A main concern of this working group was the search for an intermediate mass Higgs (i.e. $90 < m_{H^0} < 2m_W$) where the Higgs decays into $t\bar{t}$. A lot of emphasis was on the identification of top and bottom-quark jets. The interest for such Higgs signature was certainly motivated by the claim of the discovery of a top-quark with a mass of about 45 GeV. This experimental evidence has disappeared once the statistics increased. Therefore, by now (July 1986), we still consider the top-mass has a "free-parameter," only limited by the top mass being greater than 20 GeV.

[7] For a complete description of the Pythia Monte Carlo, see reference 18 an the earlier reports: H-.U. Bengtsson and G. Ingelman, Lund Preprint LUTP 84-3 and CERN TH 3820 (1984); T. Sjöstrand, Description of the Capabilities of Pythia, Contribution to the UCLA Workshop on SSC Physics, Los Angeles 1986.

[8] Description of the simulation package of the CDF Detector (see various Internal Notes of the CDF Collaboration).

[9] "Proceedings ECFA-CERN Workshop on Large Hadron Collider in the LEP Tunnel," Geneva-Lausanne, 1984 (Report ECFA 84/85,CERN 84-10), CERN, Geneva (1984)

[10] E. Eichten, I. Hinchliffe, K. Lane, C. Quigg, Rev.Mod.Phys. **56**, 579 (1984); E. Eichten, I. Hinchliffe, K. Lane, C. Quigg, Fermilab preprint FERMILAB -Pub-86/75-T.

[11] W.-K. Tung, Parton Distribution Functions Incorporating Heavy Mass Effects, to be published in the Proceedings of the Madison Workshop, May 5-16, 1986.

[12] J. Gunion and A. Savoy-Navarro, Univ.California(Davis) preprint UCD-86-11 and "Report of the W/Z/Higgs Working Group" at the UCLA Workshop on SSC Physics, Los Angeles, (Jan. 1986) page 338. The interest to study the process

$H^0 \to ZZ$, looking at the decay channel:$Z \to ll$ ($l = e$ or μ), and $Z \to \nu\bar{\nu}$, has been emphasized at the UCLA meeting by M.S. Chanowitz, "Weak Interactions at the SSC," LBL Preprint:LBL-21290 and published in the Proceedings of the UCLA Workshop page 183. In fact this signature was already pointed out by M.S. Chanowitz and M.K. Gaillard (see Ref 26) and has been studied in more details by: R. Cahn and M. Chanowitz, Phys. Rev. Lett. **56**, 1327 (1986) and M.S. Chanowitz, "W,Z Scattering Theorems and No-lose Corollary for SSC" to be published in the Proceedings of the XXIII International Conference on High Energy Physics, Berkeley, Cal., July 16-23, 1986.

[13] Standard charged Higgs' also give some experimental hints to look for a non-standard Higgs although in this report we have only considered the problem of how to detect a "conventional Higgs."

[14] The experimental evidence for the tau-signal produced in pp collisions has been given for the first time by the UA1 collaboration. The events produced by the leptonic decay of the W to $\tau\nu_\tau$ appear to be the major standard contribution to the events characterized by jet(s) and missing energy; A. Savoy-Navarro, contribution to the "Proc. 5th Topical Workshop on Proton-Antiproton Collider Physics" St.Vincent, 1985, page 196. C. Albajar et al., UA1 Collaboration, paper in preparation.

[15] F.E. Paige, S.P. Protopopescu, Isajet M.C., BNL-29777, Brokhaven, 1983 and BNL-37271, August(1985), "ISAJET 5.02;A Monte Carlo Generator for pp and $p\bar{p}$ Interactions."

[16] For a survey of soft gluon theory see: A. Bassetto, M. Ciafalloni and G. Marchesini, Phys. Rep. **100**, 202 (1983) and the contribution of G. Marchesini "Infrared Problem in QCD," page 88 and, "Comments on Monte-Carlo codes for QCD cascade" page 114, in Proceedings of the UCLA Workshop on "Observable Standard Model Physics at the SSC:Monte Carlo Simulation and Detector Capabilities," Los Angeles, (Jan 1986). For a discussion of this problem from the Monte-Carlo point of view see in the UCLA Proceedings: T. Gottschalk, "A New Model for Coherent Final State Parton Showers," page 122; T. Sjöstrand, "Comments on Initial State Radiation and Multiple Interactions," page 38; F. Paige, "Prospects for SSC physics," page 372.

[17] A. Savoy-Navarro, "Experimental Searches for W Pairs and Higgs at a high energy pp collider," contribution to the Proceedings of the Madison Workshop, on "Physics Simulations at High Energy," Madison, May 5-16, 1986 and references therein.

[18] H.-U. Bengtsson, T. Sjöstrand, these proceedings.

[19] M.S. Chanowitz, M.K. Gaillard, Nuclear Physics **B261**, 379 (1985).

[20] J. F. Gunion, H. E. Haber, F. Paige, W.-K. Tung, S. S. D. Willenbrock, UC Davis preprint UCD-86-15 (1986).

[21] D. Duke, J. F. Owens, Phys. Rev. **D30** (1984) 49.

[22] M. Glück, E. Hoffman, E. Reya, Z. Physik **C13** (1982) 119.

[23] J. C. Collins, W.-K. Tung, Fermilab preprint FERMILAB-Pub-86/39-T (1986); W.-K. Tung, Parton Distribution Functions Incorporating Heavy Mass Effects, to be published in Proceedings of the Madison Workshop, May 5–16, 1986.

[24] S. Dawson and A. Savoy-Navarro, Report of the Working Group "Searching for Supersymmetry at the SSC," Proceedings of the Summer Study on the Design and Utilization of the Superconducting Super Collider, Snowmass, Colo., 1984.

[25] Proc. Workshop on Triggering, Data Acquisition and Offline Computing for High Energy/High Luminosity Hadron-Hadron Collider, Batavia, Ill., 1985, page 1.

[26] M.S. Chanowitz, M.K. Gaillard, Phys. Lett. **142B**, 85 (1984); also reference 19.

Figure 2.1: Pictures of events: $p\bar{p} \rightarrow W \rightarrow W + H^0$ or $p\bar{p} \rightarrow Z^0 \rightarrow Z^0 + H^0$, generated by Pythia at $\sqrt{s}$= 2 TeV and passed through the CDF simulation; Higgs masses of a) 20 GeV, b) 50 GeV, and c) 70 GeV. In each case, $H^0 \rightarrow \tau^+\tau^-$, $W \rightarrow q\bar{q}$ and $Z^0 \rightarrow \nu\bar{\nu}$.

Figure 2.2: Pictures of events: $pp \rightarrow W \rightarrow W + H^0$ or $pp \rightarrow Z^0 \rightarrow Z^0 + H^0$, generated by Pythia at $\sqrt{s}$= 10 TeV and passed through the CDF simulation; Higgs masses of a) 50 GeV, and b) 100 GeV. In each case, $H^0 \rightarrow \tau^+\tau^-$, $W \rightarrow q\bar{q}$ and $Z^0 \rightarrow \nu\bar{\nu}$.

Figure 2.3: The cross section to produce a H^0 with a mass of 300 GeV (solid line) or 400 GeV (dashed line) as a function of $\sqrt{s}$ for: a) an e^+e^- collider, b) an ep collider and, c) a pp collider.
Fig. 2.4: Feynman diagrams for the processes a) ep → WW by W fusion
b) ep → WW by $\gamma\gamma$ mechanism
Figure 2.5: WW invariant mass distribution for the process $ep \rightarrow H^0 \rightarrow WW$ for m_{H^0}= 200, 300 and 400 GeV at $\sqrt{s}$ = 1 TeV. The contribution due to WW fusion (solid line) is separated from the $\gamma\gamma$ fusion (dashed line).

Figure 2.6: WW invariant mass distribution for the process $ep \rightarrow H^0 \rightarrow WW$ for m_{H^0}= 200, 300 and 400 GeV at $\sqrt{s}$ = 3 TeV. The contribution due to WW fusion (solid line) is separated from the $\gamma\gamma$ fusion (dashed line).

Figure 2.7: Pictures of events: $pp \rightarrow H^0 \rightarrow WW$ at $\sqrt{s}$= 10 TeV with m_{H^0}= 200 GeV generated by Pythia and passes through the CDF simulation. In each case, one $W \rightarrow q\bar{q}$ and the other goes by $W \rightarrow e\nu_e$.

Figure 2.8: Higgs mass range accessible to all the machines either built or going to be built by the end of this century.

Figure 4.1: The angle between the 2 W's (decay products of the Higgs) as generated by the Pythia M.C. for a Higgs mass of a) 300 GeV and b) 800 GeV.

Figure 4.2: The azimuthal angle between the two jets produced by the hadronic decay of one of the W's (from a Higgs decay) for a Higgs mass of a) 300 GeV and b) 800 GeV.

Figure 4.3: Displays of a minimum bias event as generated by the pythia M.C. showing: a) the momenta of the 2 produced gluons in a 3D view; b) reconstructed jets in the event in a 3d view; c) LEGO plot of the event; d) transverse view showing all charged tracks, no B-field (leptons are dashed lines); e) 3D view of all charged tracks with a solenoidal B-field (1.5 tesla).

Figure 4.4: Displays of a 1 TeV QCD event as generated by the pythia M.C. showing: a) the momenta of the 2 gluons in a 3D view; b) 3D view of all charged tracks with a solenoidal B-field (1.5 tesla). It shows a clear 2 high-p_t jet structure.

Figure 4.5: Displays of $H^0 \rightarrow WW$ event with Higgs mass of 300 GeV and $W \rightarrow e\nu$ and $W \rightarrow q\bar{q}$ as generated by the pythia M.C. showing: a) the momenta of the 2 W's in a 3D view; b) reconstructed jets in the event in a 3d view; c) leptons in the event; d) transverse view showing all charged tracks, no B-field (leptons are dashed lines); e) 3D view of all charged tracks with a solenoidal B-field (1.5 tesla).

Figure 4.6: Displays of $H^0 \rightarrow ZZ$ event with Higgs mass of 300 GeV and $Z \rightarrow l^+l^-$ and $Z \rightarrow \nu\overline{\nu}$ as generated by the pythia M.C. showing: a) the momenta of the 2 Z's in a 3D view; b) reconstructed jets in the event in a 3d view; c) leptons in the event in a 3D view; d) transverse view showing all charged tracks, no B-field (leptons are dashed lines); e) 3D view of all charged tracks with a solenoidal B-field (1.5 tesla).

Figure 4.7: Displays of $H^0 \rightarrow WW$ event with Higgs mass of 800 GeV and $W \rightarrow \mu\nu$ and $W \rightarrow q\overline{q}$ as generated by the pythia M.C. showing: a) the momenta of the 2 W's in a 3D view; b) reconstructed jets in the event in a 3d view (16 jets with $E_T > 10$ GeV); c) leptons in the event (2 high-p_t leptons in addition to the muon from the W-decay); d) transverse view showing all charged tracks, no B-field (leptons are dashed lines); e) 3D view of all charged tracks with a solenoidal B-field (1.5 tesla).

Figure 4.8: Displays of $H^0 \rightarrow ZZ$ event with Higgs mass of 800 GeV and $Z \rightarrow l^+l^-$ and $Z \rightarrow \nu\overline{\nu}$ as generated by the pythia M.C. showing: a) the momenta of the 2 Z's in a 3D view; b) reconstructed jets in the event in a 3d view; c) leptons in the event in a 3D view (the 2 leptons from the Z are quite central and collimated); d) transverse view showing all charged tracks, no B-field (leptons are dashed lines); e) 3D view of all charged tracks with a solenoidal B-field (1.5 tesla). Note that there are extra high-p_t leptons in addition to those from the Z.

Figure 4.9: Missing energy distributions for ZZ continuum events with: a) $100 < p_{tZ} < 200$ GeV; b) $300 < p_{tZ} < 400$ GeV; c) $500 < p_{tZ} < 600$ GeV.

Figure 4.10: Schema of the trigger strategies for W-pairs.

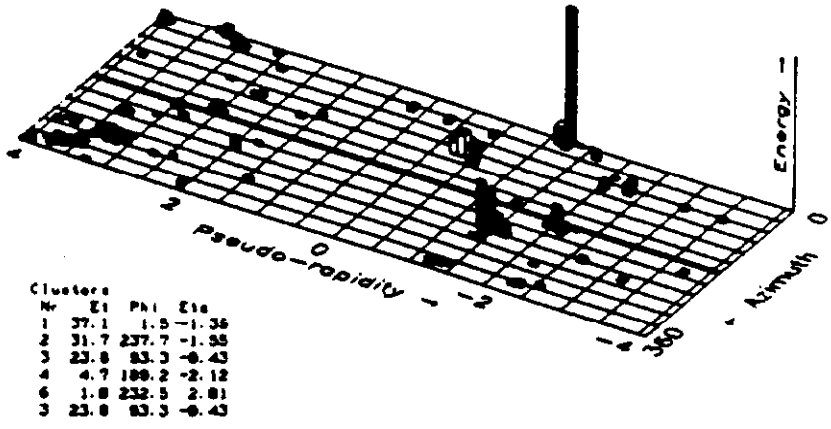

a) E_T^{miss} = 18.4 GeV

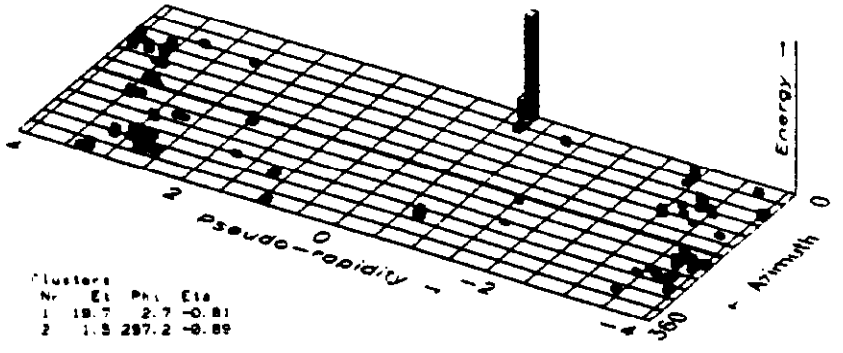

b) E_T^{miss} = 21.2 GeV

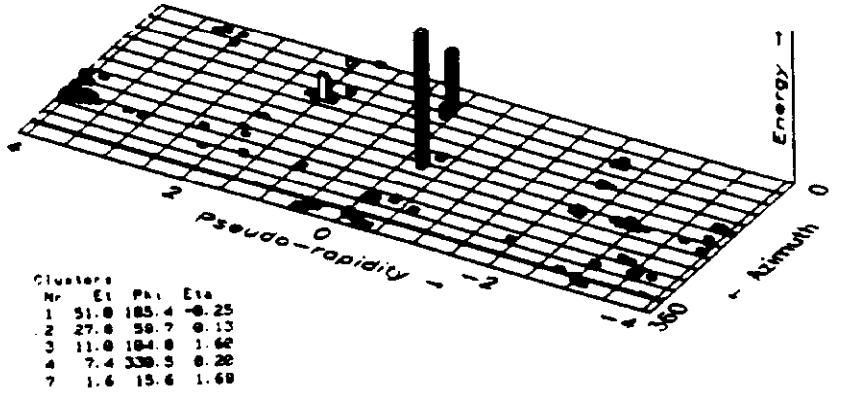

c) E_T^{miss} = 39.5 GeV

Fig. 2.1

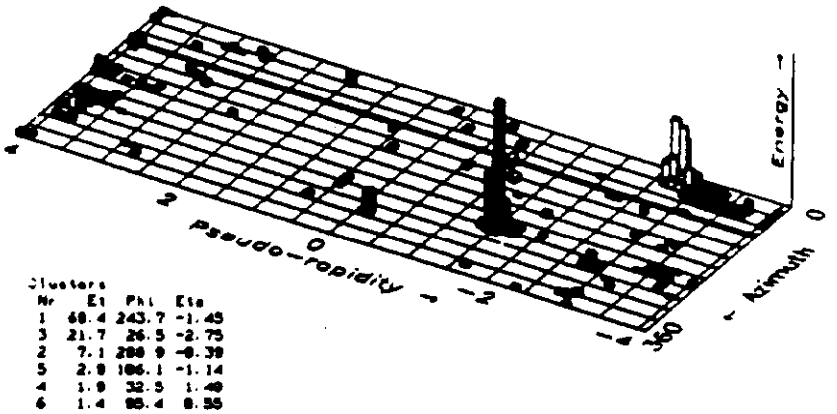

Clusters

Nr	Et	Phi	Eta
1	60.4	243.7	-1.45
3	21.7	26.5	-2.75
2	7.1	288.9	-0.39
5	2.8	186.1	-1.14
4	1.8	32.5	1.40
6	1.4	98.4	0.55

c) E_T^{miss} = 53.6 GeV

Fig. 2.1 cont'd

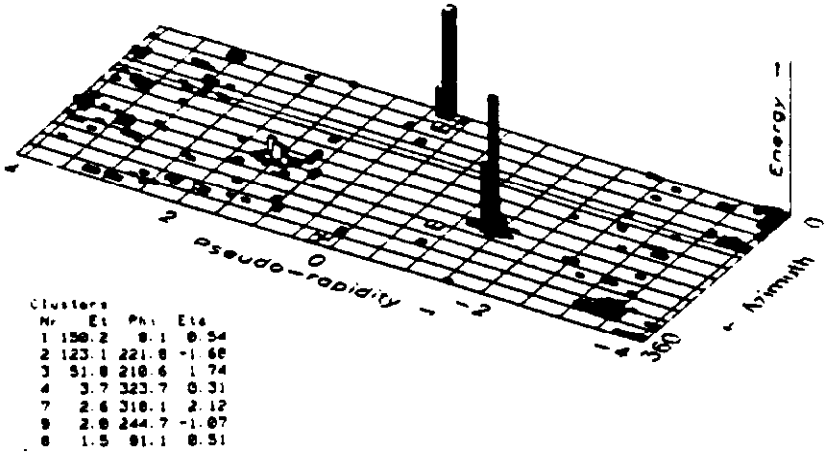

Clusters

Nr	Et	Phi	Eta
1	150.2	0.1	0.54
2	123.1	221.8	-1.60
3	91.8	210.6	1.74
4	3.7	323.7	0.31
7	2.6	310.1	2.12
9	2.0	244.7	-1.07
8	1.5	91.1	0.51

a) E_T^{miss} = 102.6 GeV

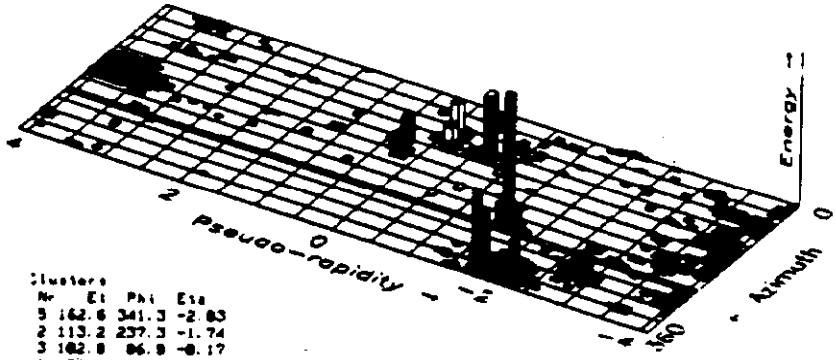

Clusters

Nr	Et	Phi	Eta
5	162.6	341.3	-2.83
2	113.2	237.3	-1.74
3	102.8	86.9	-0.17
1	81.4	113.6	-0.84
4	52.6	136.8	0.34
6	28.6	287.5	-2.84
11	4.4	38.1	-1.42
10	3.7	25.5	-0.48

b) E_T^{miss} = 64.5 GeV

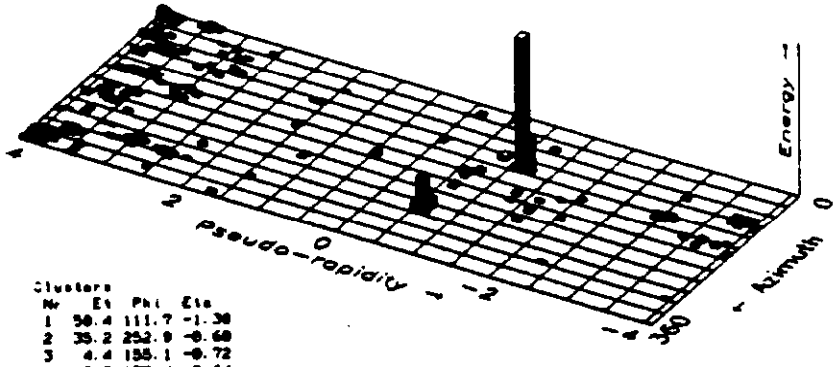

Clusters

Nr	Et	Phi	Eta
1	58.4	111.7	-1.38
2	35.2	252.9	-0.68
3	4.4	155.1	-0.72
4	2.8	178.4	0.64

b) E_T^{miss} = 47.0 GeV

Fig. 2.2

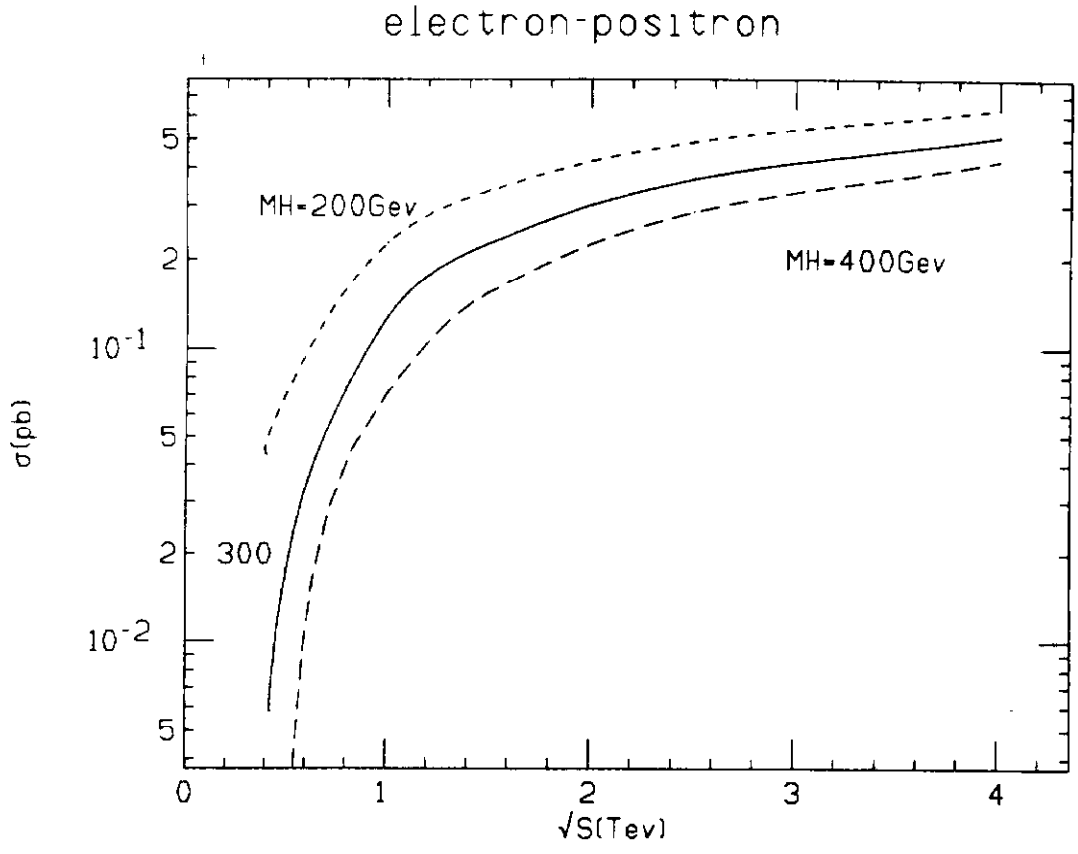

Figure 2.3 (a)

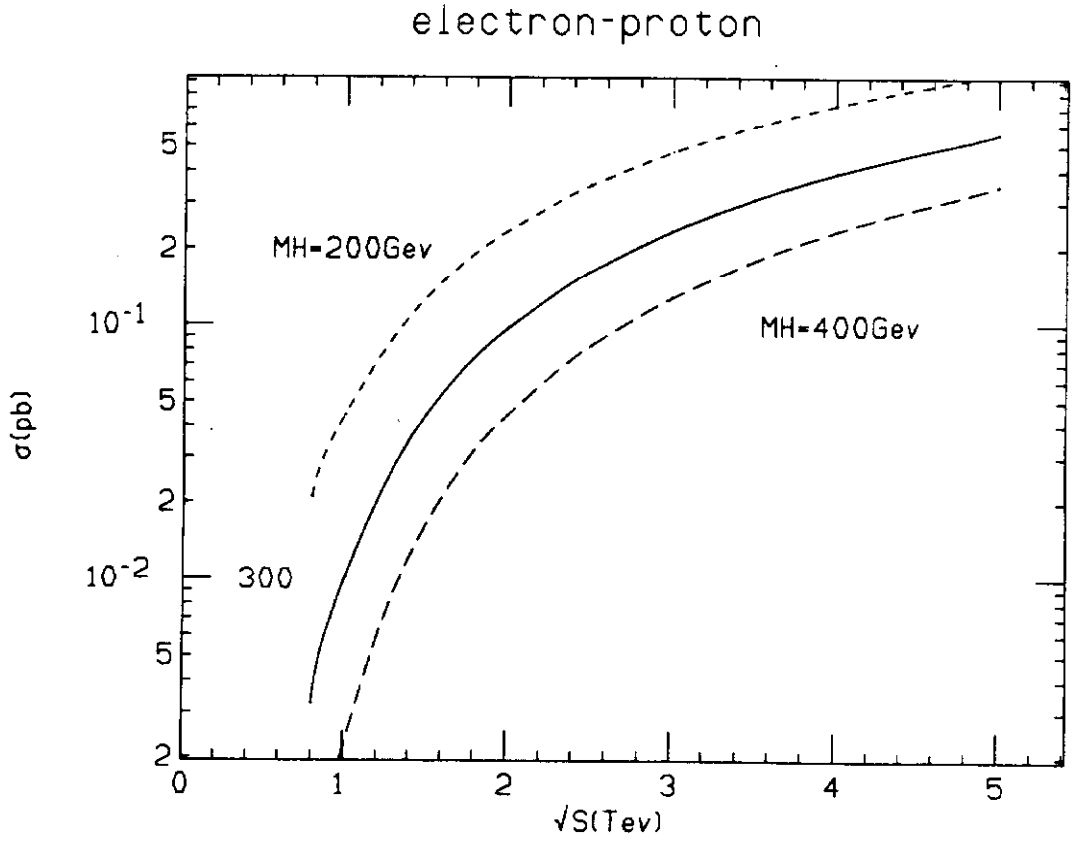

Figure 2.3 (b)

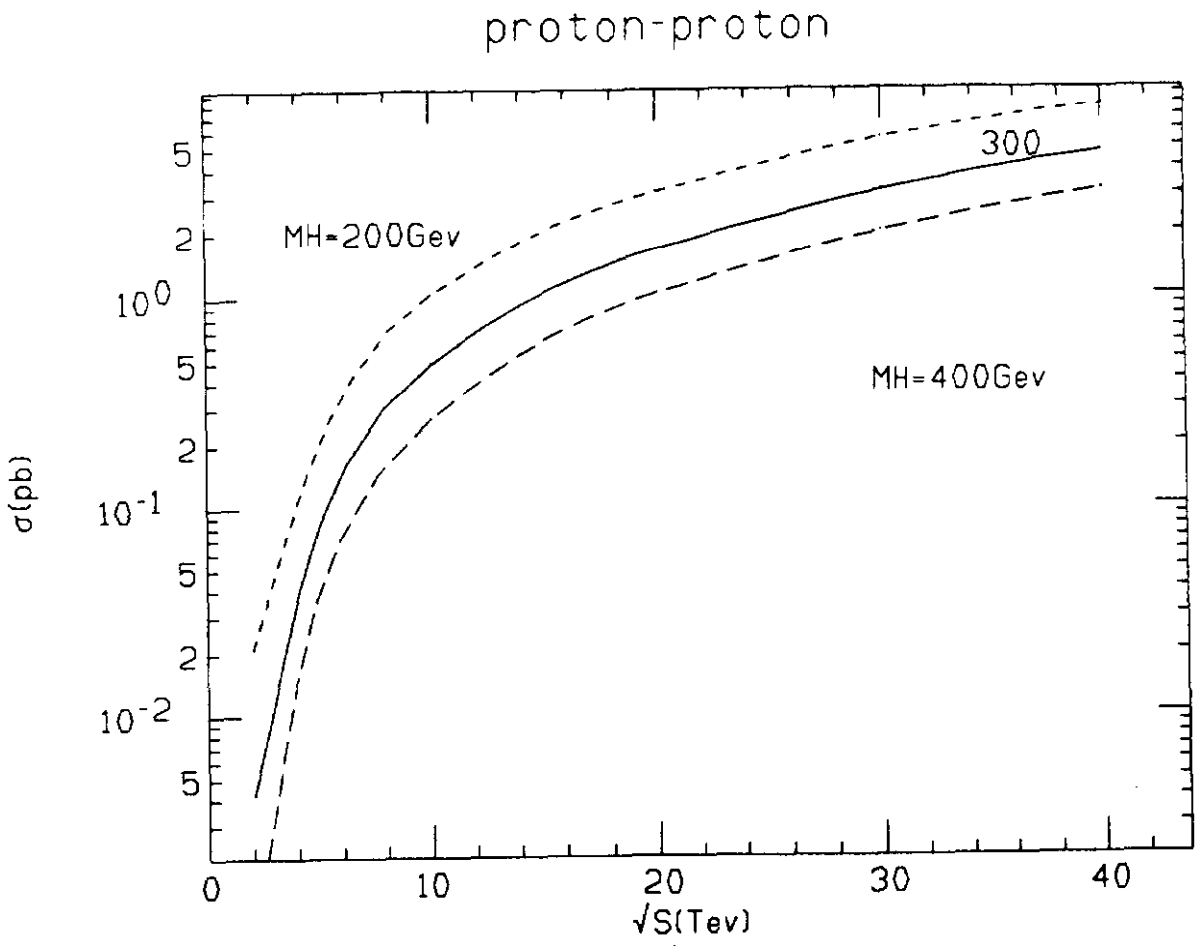

Figure 2.3 (c)

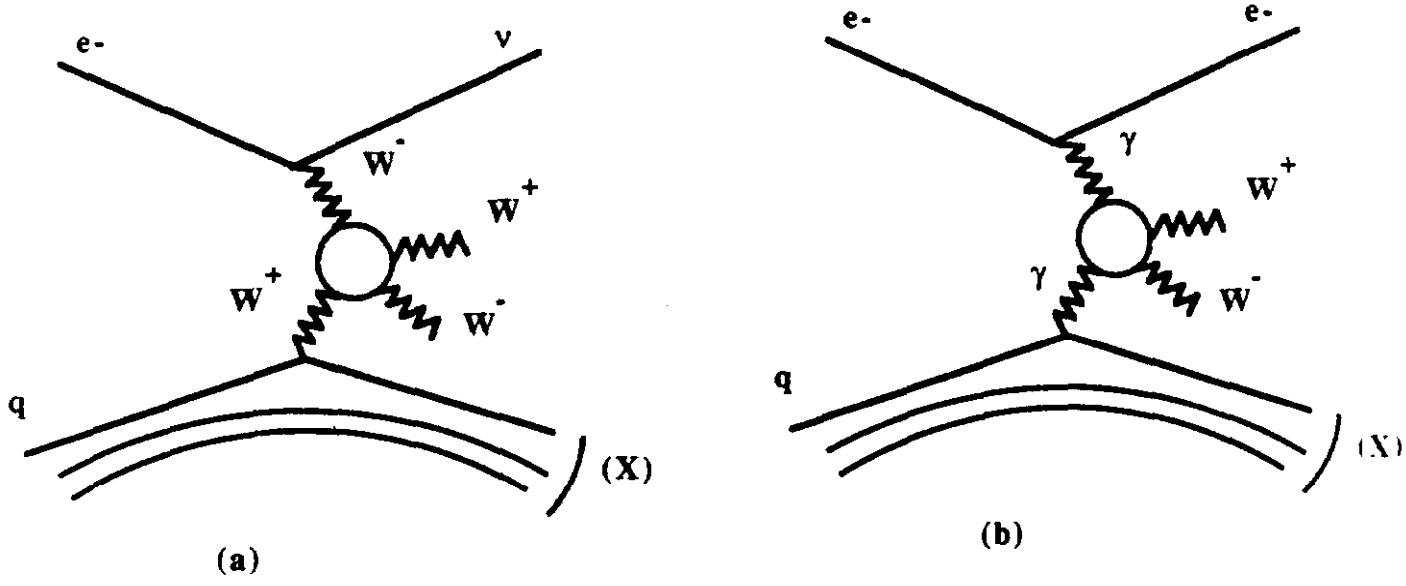

Figure 2.4

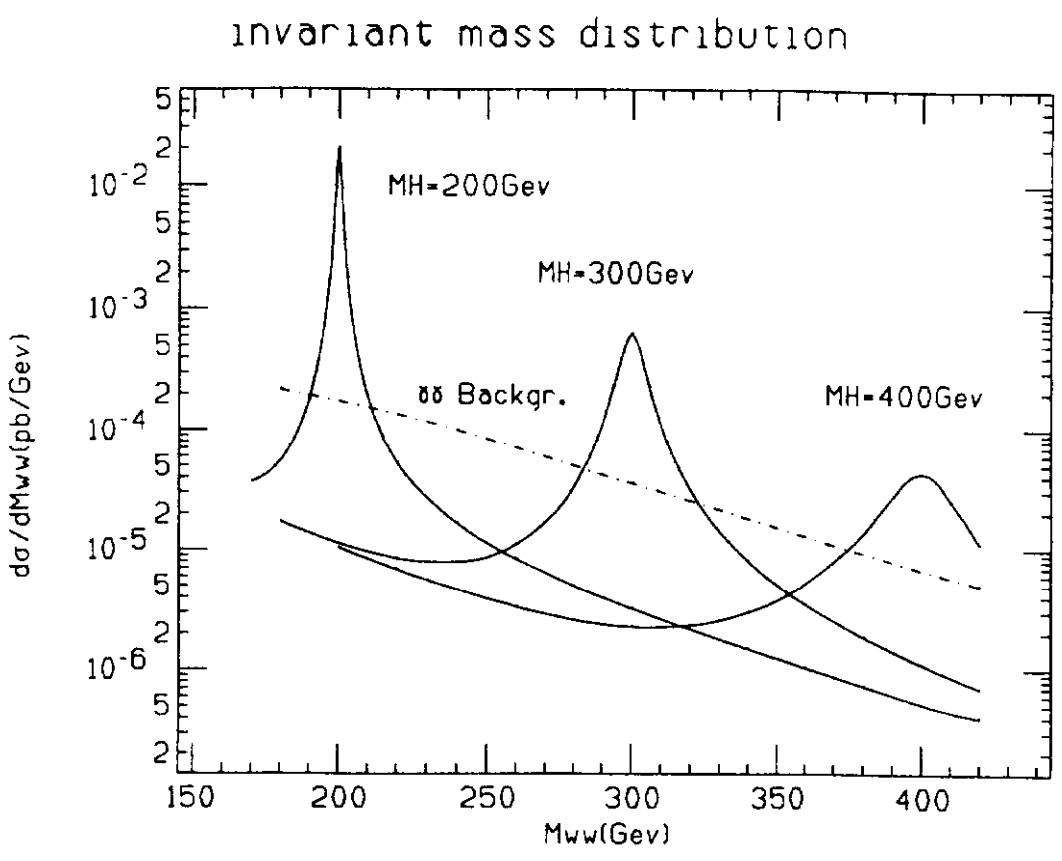

Figure 2.5

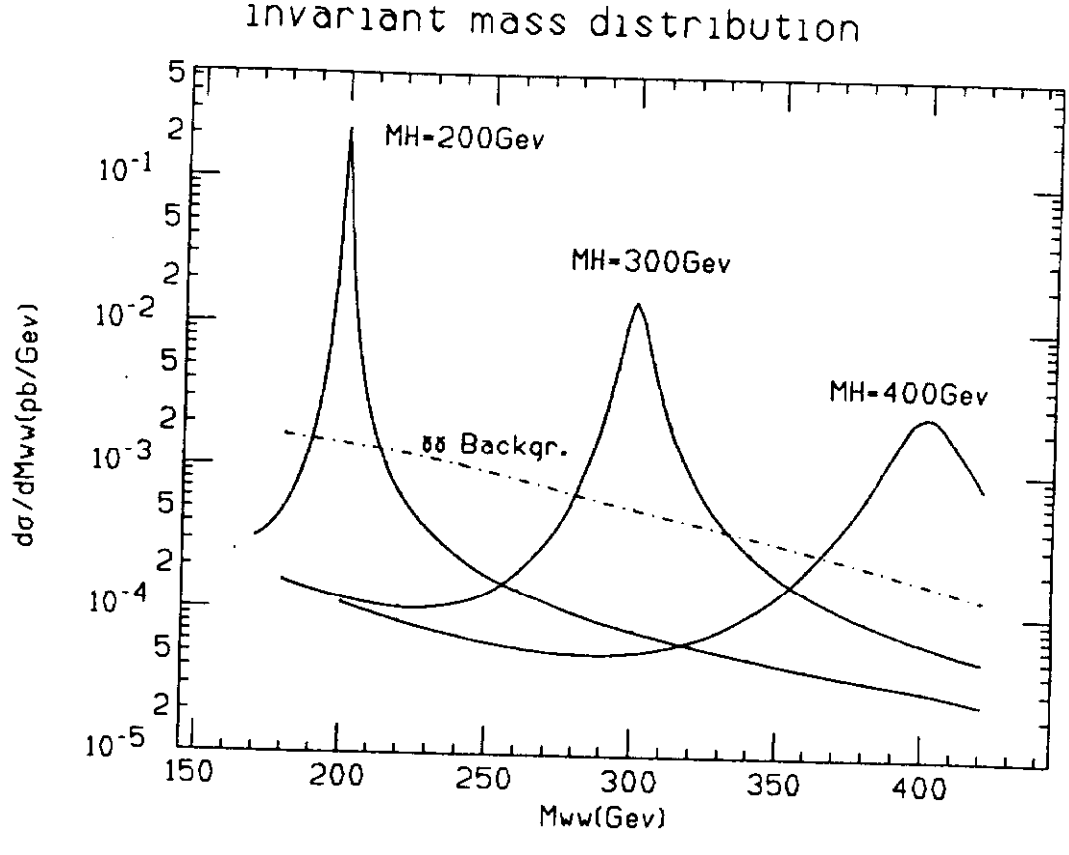

Figure 2.6

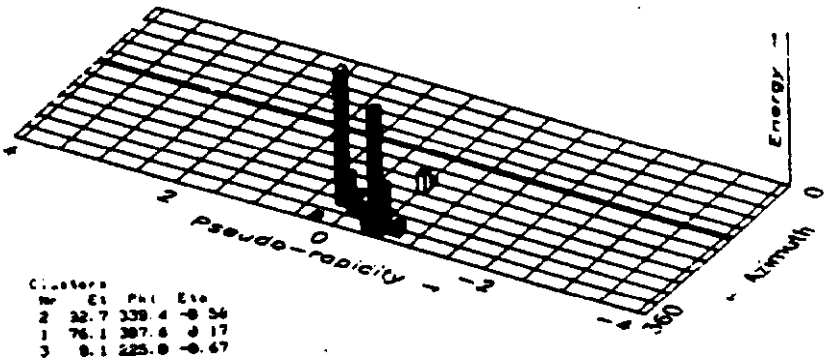

Clusters

Nr	Et	Phi	Eta
2	32.7	339.4	-0.56
1	76.1	307.6	0.17
3	8.1	225.0	-0.67

E_T^{miss} = 162 GeV

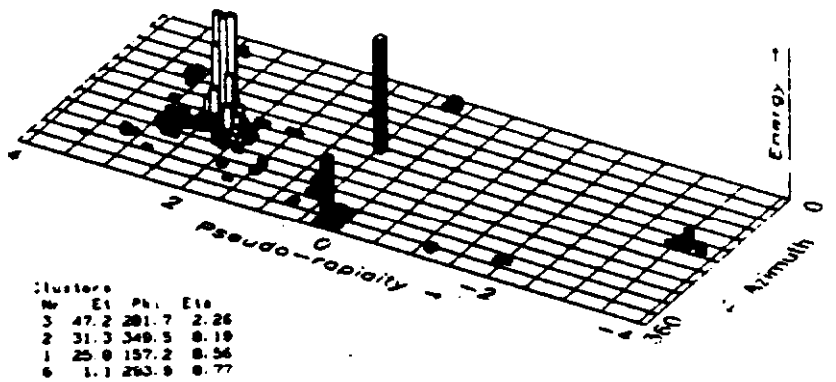

Clusters

Nr	Et	Phi	Eta
5	47.2	281.7	2.26
2	31.3	349.5	0.19
1	25.0	157.2	0.56
6	1.1	263.9	0.77

E_T^{miss} = 49.5 GeV

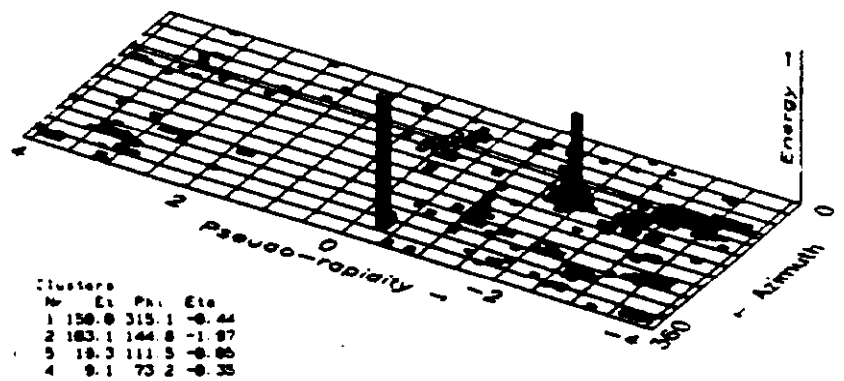

Clusters

Nr	Et	Phi	Eta
1	150.0	315.1	-0.44
2	183.1	144.8	-1.87
5	19.3	111.5	-0.86
4	9.1	73.2	-0.35
7	7.2	261.5	-2.20
10	6.0	240.4	-1.26
8	2.3	182.9	-1.14
11	2.0	43.6	-1.87

E_T^{miss} = 23.1 GeV

Fig. 2.7

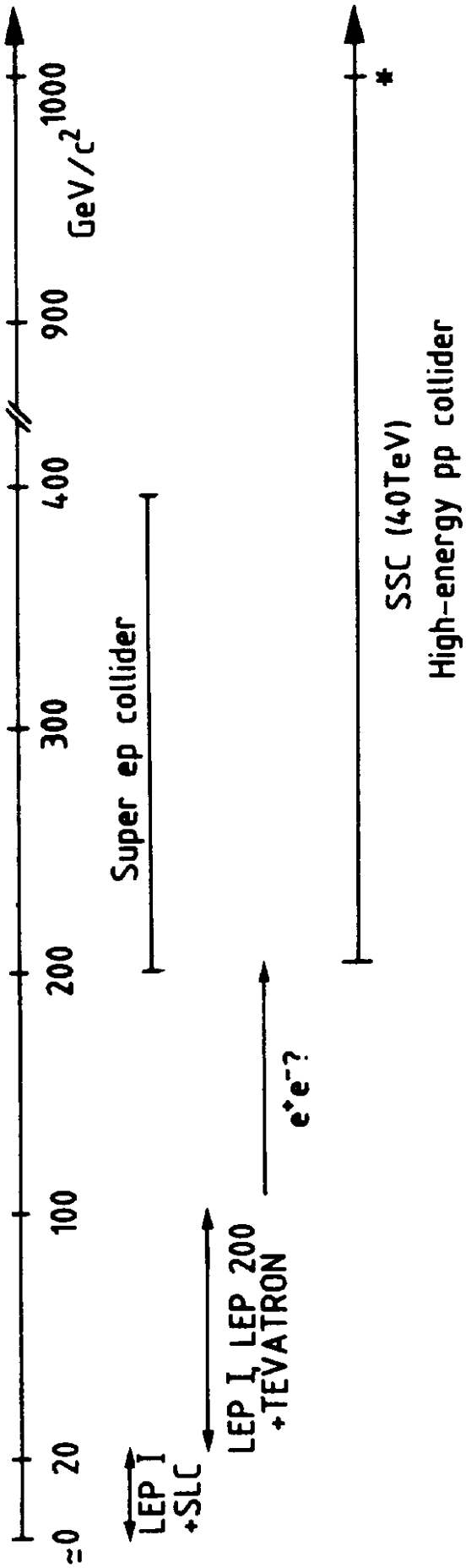
≃0
20
100
200
300
400
900
1000
GeV/c²
LEP I
+SLC
LEP I, LEP 200
+TEVATRON
e⁺e⁻?
Super ep collider
SSC (40TeV)
High-energy pp collider

Figure 2.8

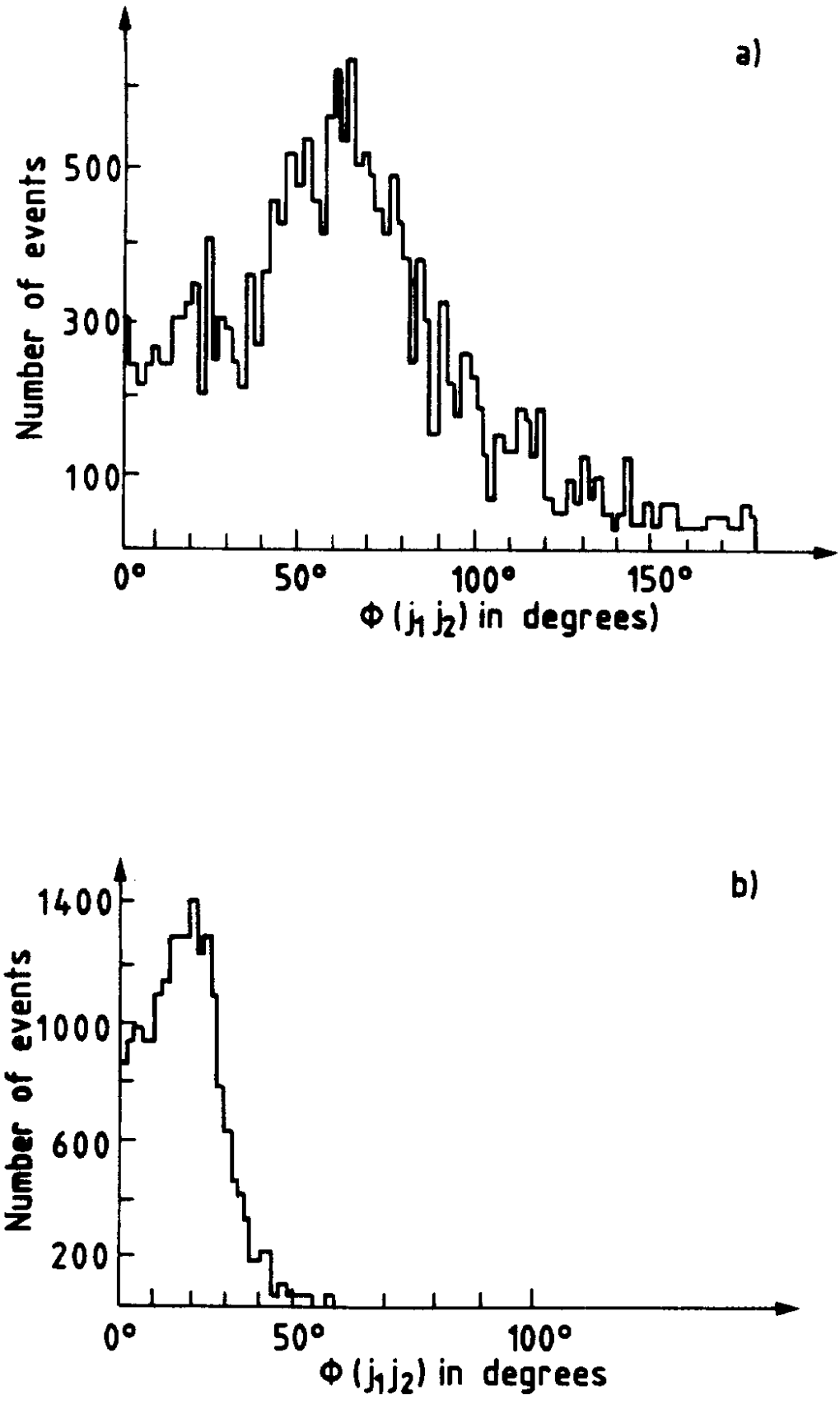
a)
Number of events
500
300
100
0°
50°
100°
150°
Φ (j1 j2) in degrees)
b)
Number of events
1400
1000
600
200
0°
50°
100°
Φ (j1j2) in degrees

Figure 4.1

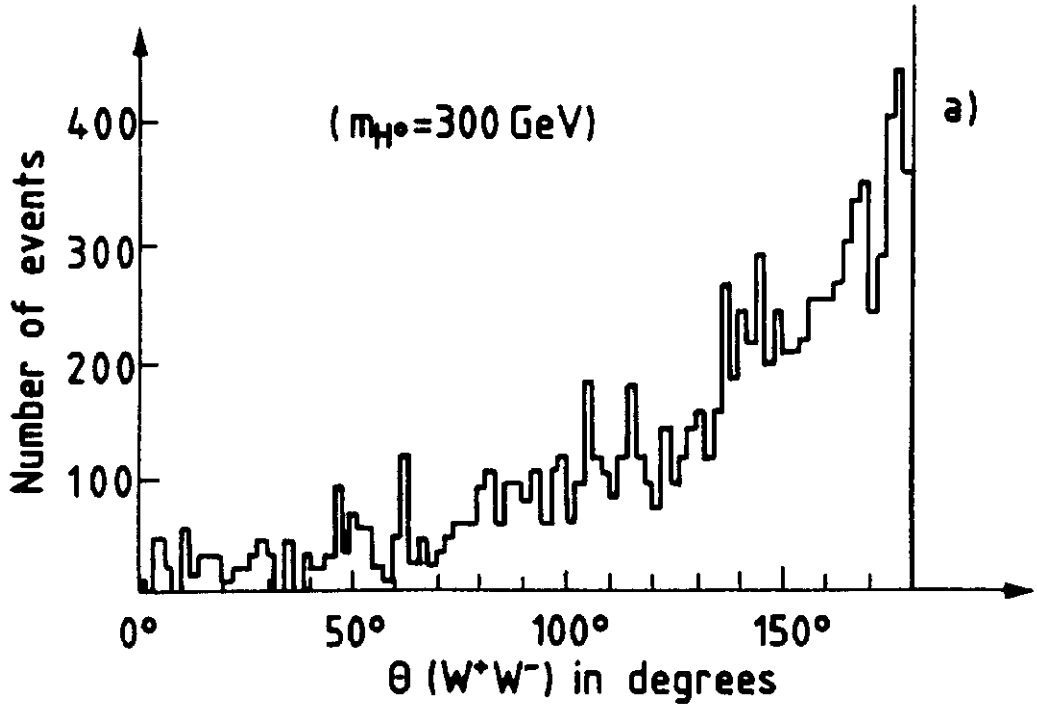
(m$_{H^0}$=300 GeV)
a)
Number of events
400
300
200
100
0°
50°
100°
150°
θ (W⁺W⁻) in degrees

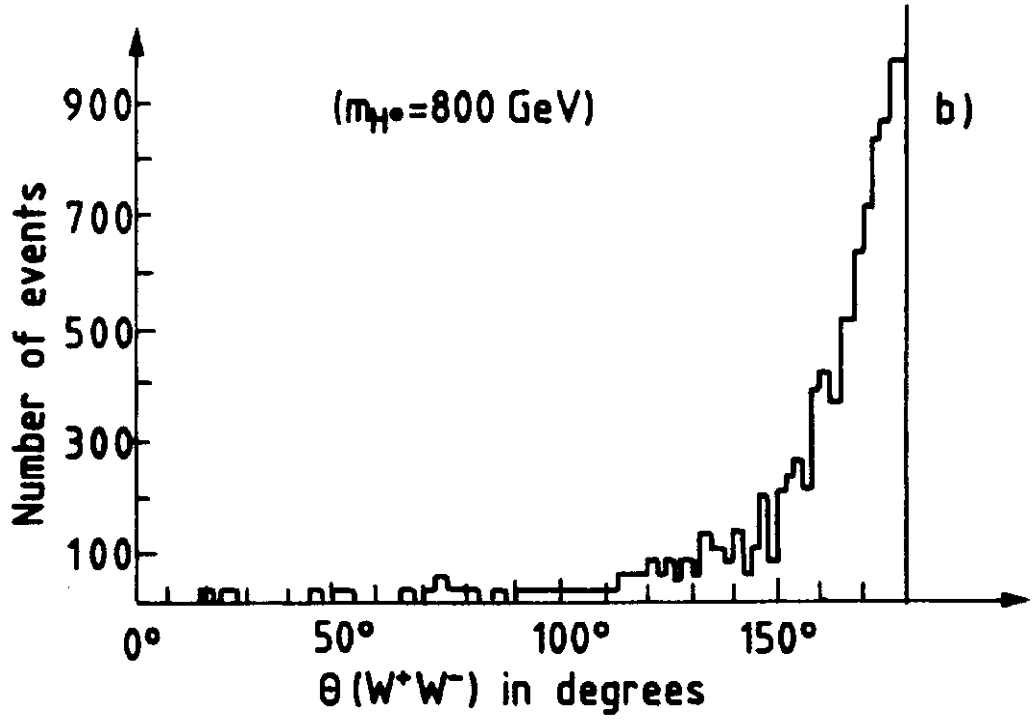
(m$_{H^0}$=800 GeV)
b)
Number of events
900
700
500
300
100
0°
50°
100°
150°
θ (W⁺W⁻) in degrees

Figure 4.2

LO PT QCD

ID	TK	PT	PZ	P	THET	PHI
GL	P 1	13.1	1.5	13.2	83.5	41.7
GL	P 2	4.6	-100.5	100.6	177.4	-104.3

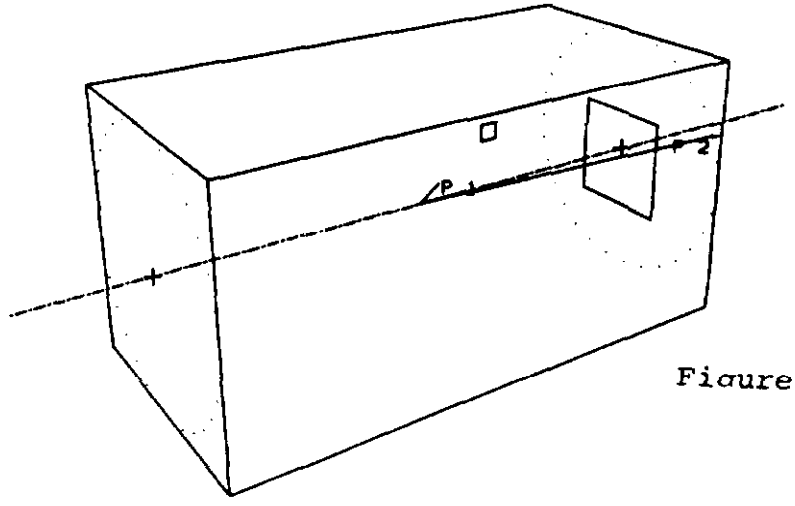

Figure 4.3 (a)

LO PT QCD

ID	TK	PT	PZ	P	THET	PHI
	J 1	9.1	-5.7	10.7	121.8	107.0
	J 2	8.5	28.3	29.6	16.7	-166.6
	J 3	8.5	-2.6	8.9	106.8	43.6
	J 4	7.4	9.3	11.8	38.5	-81.6

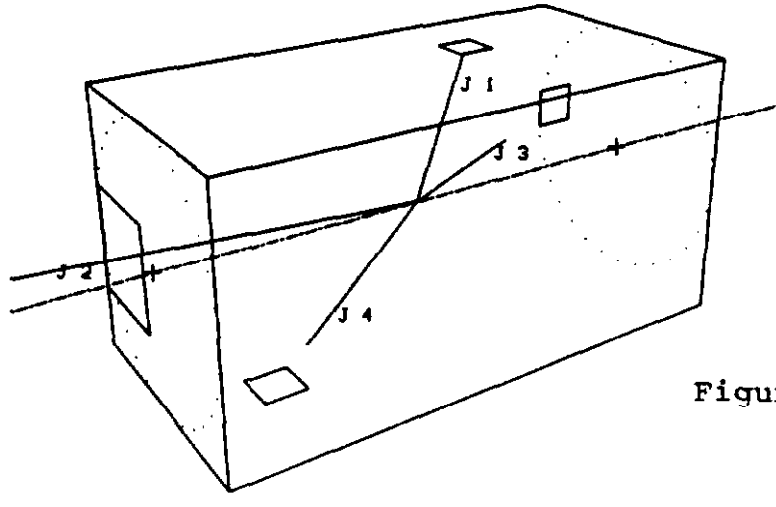

Figure 4.3 (b)

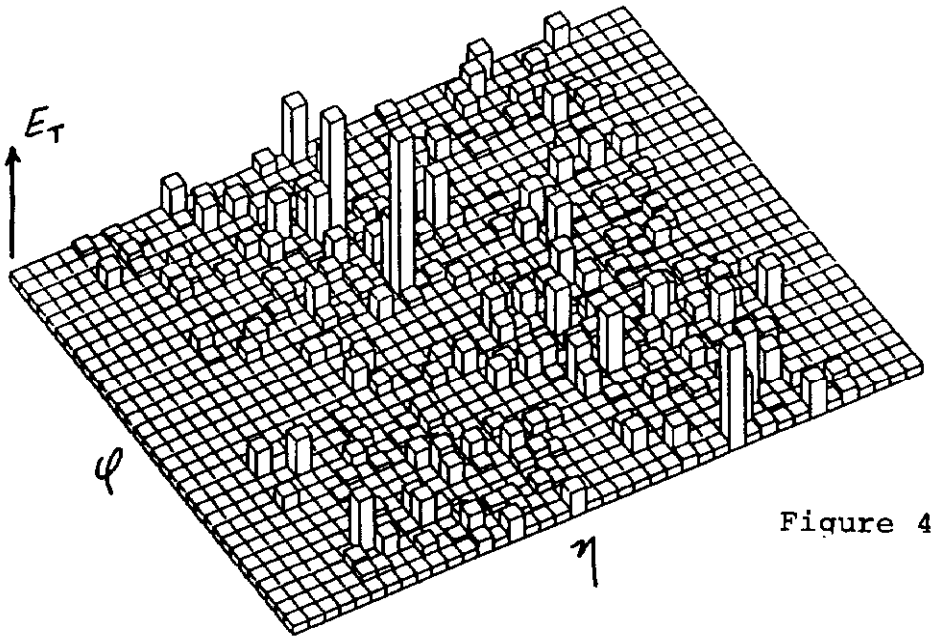

Figure 4.3 (c)

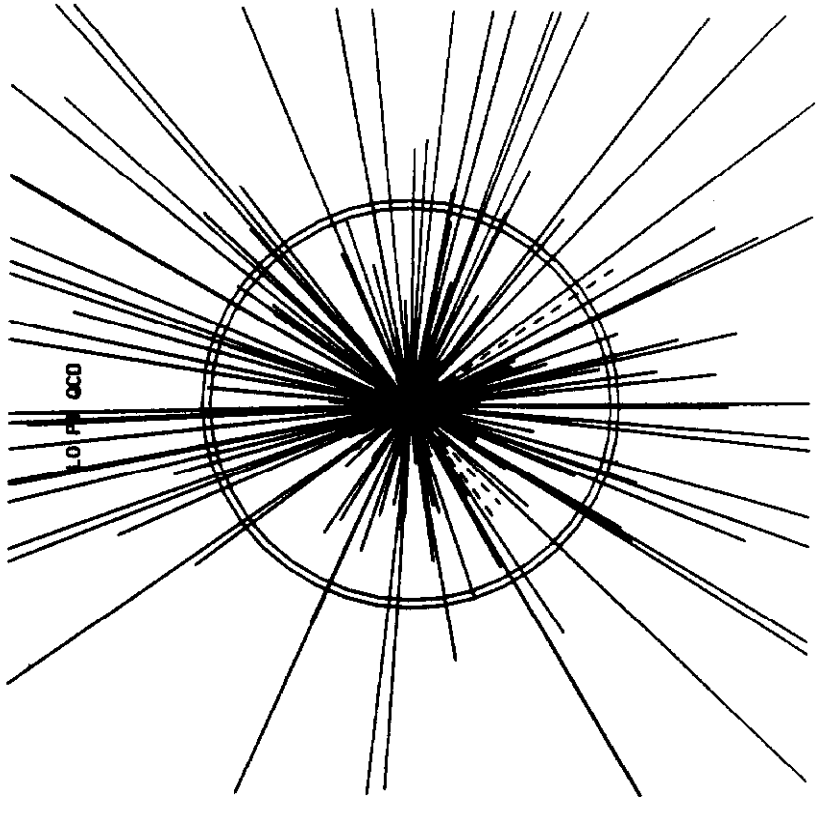

Figure 4.3 (d)

LO PT QCD

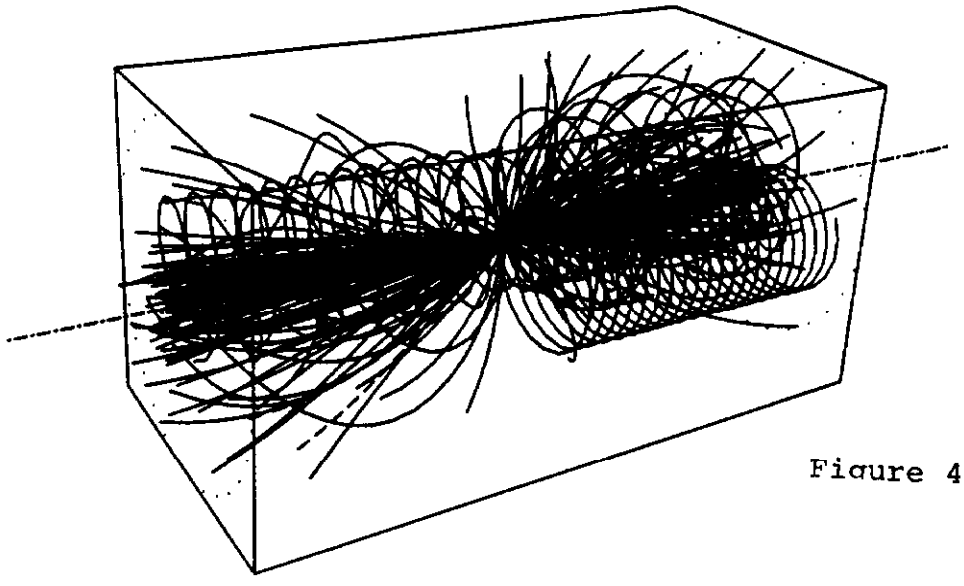

Figure 4.3 (e)

1 TEV PT QCD

ID	TK	PT	PZ	P	THET	PHI
GL	P 1	1079.6	-560.5	1216.4	117.4	-71.1
GL	P 2	1119.9	-5332.6	5448.9	168.1	110.5

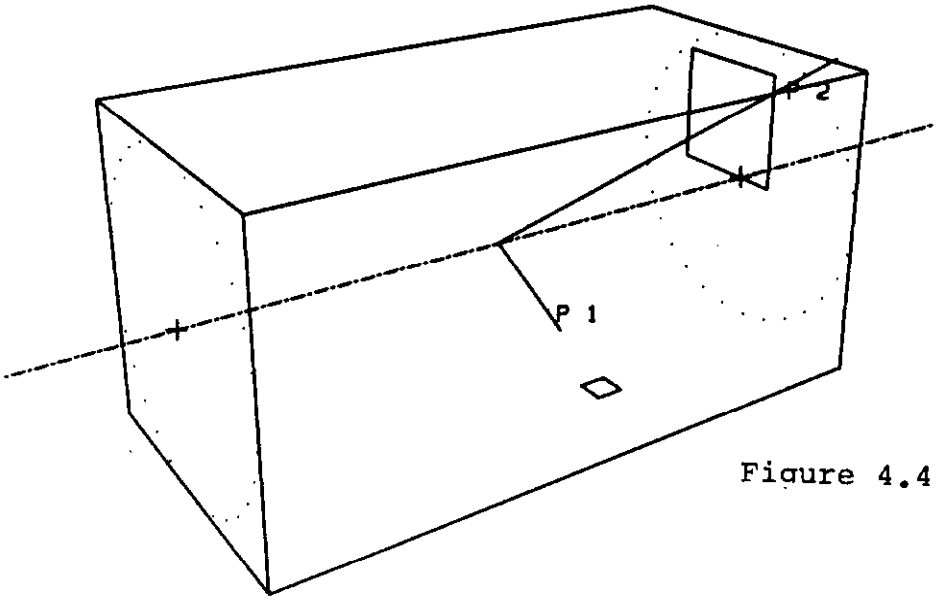

Figure 4.4 (a)

1 TEV PT QCD

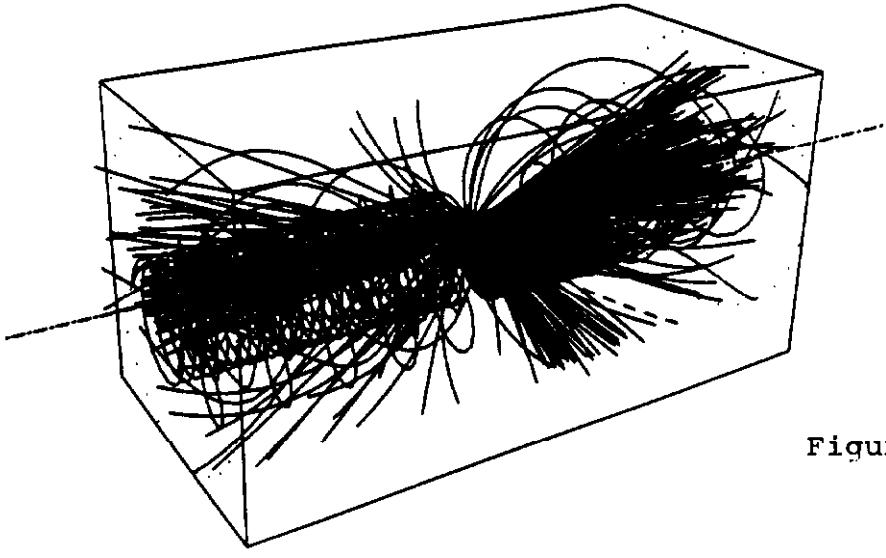

Figure 4.4 (b)

HWW300

	ID	TK	PT	PZ	P	THET	PHI
W-		P 1	72.3	-266.8	276.2	164.8	39.8
W+		P 2	188.4	-896.0	915.6	168.1	150.1

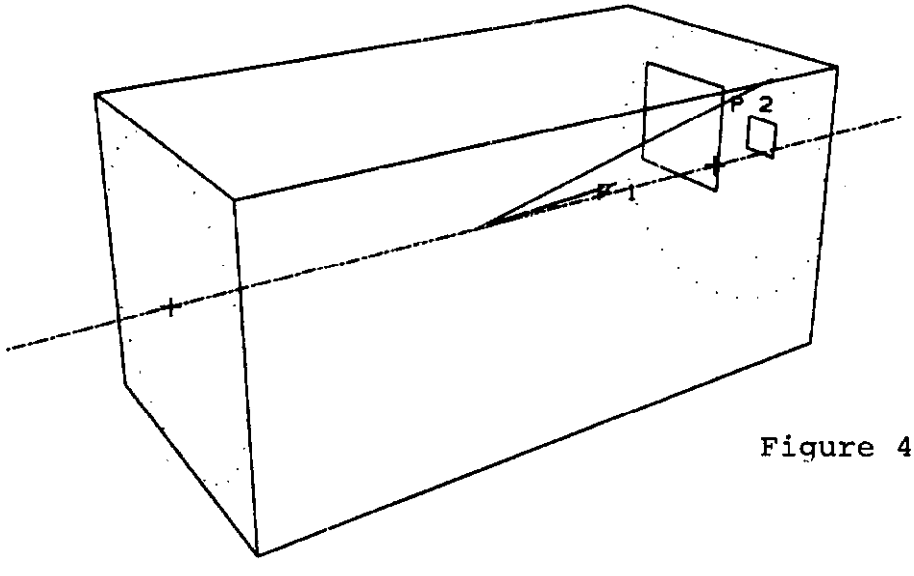

Figure 4.5 (a)

HWW300

ID	TK	PT	PZ	P	THET	PHI
	J 1	137.8	-440.0	461.1	162.6	42.1
	J 2	97.5	349.2	362.6	15.6	-55.4
	J 3	91.6	820.8	825.9	6.4	-24.0
	J 4	80.4	-129.7	152.6	148.2	-164.5
	J 5	49.8	-336.7	340.3	171.6	112.5
	J 6	32.4	-111.8	116.5	163.8	14.3
	J 7	30.5	-87.4	92.6	160.8	-139.4
	J 8	24.3	132.3	134.5	10.4	-50.0

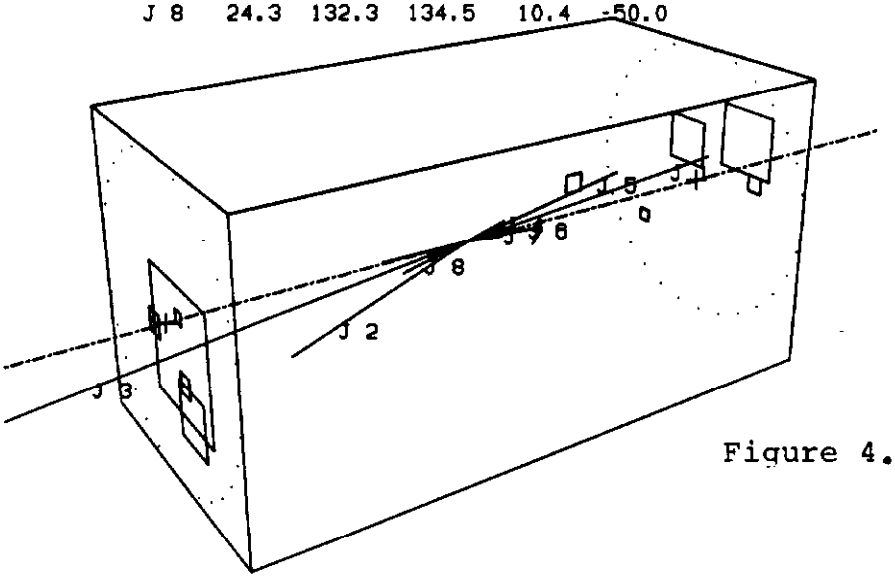

Figure 4.5 (b)

HWW300

ID	TK	PT	PZ	P	THET	PHI
E+	1	46.9	-309.3	312.8	171.4	112.8
NUE	2	153.7	-586.8	606.6	165.3	180.8
MU-	353	0.1	0.3	0.3	21.6	77.6
ANUM	354	1.7	2.2	2.7	37.9	-62.2
	MISS	147.8				161.0

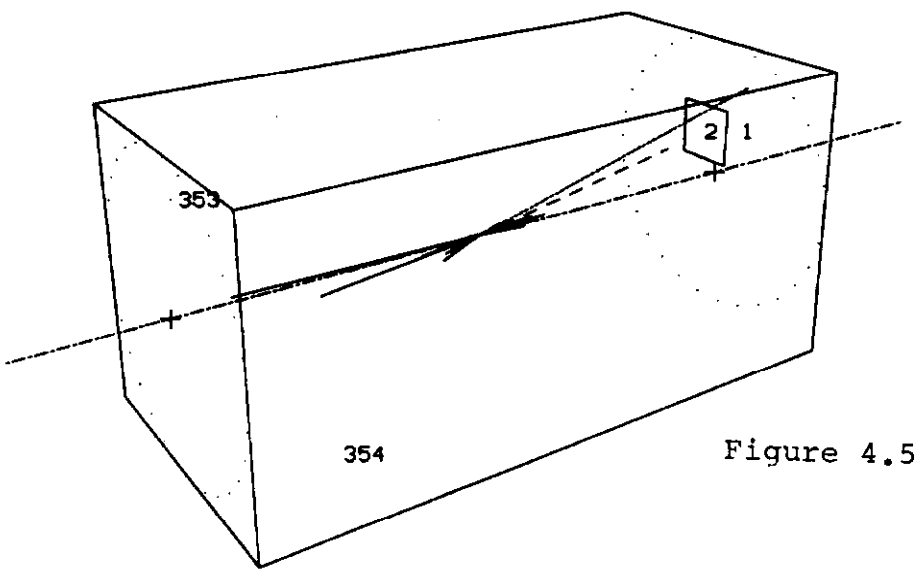

Figure 4.5 (c)

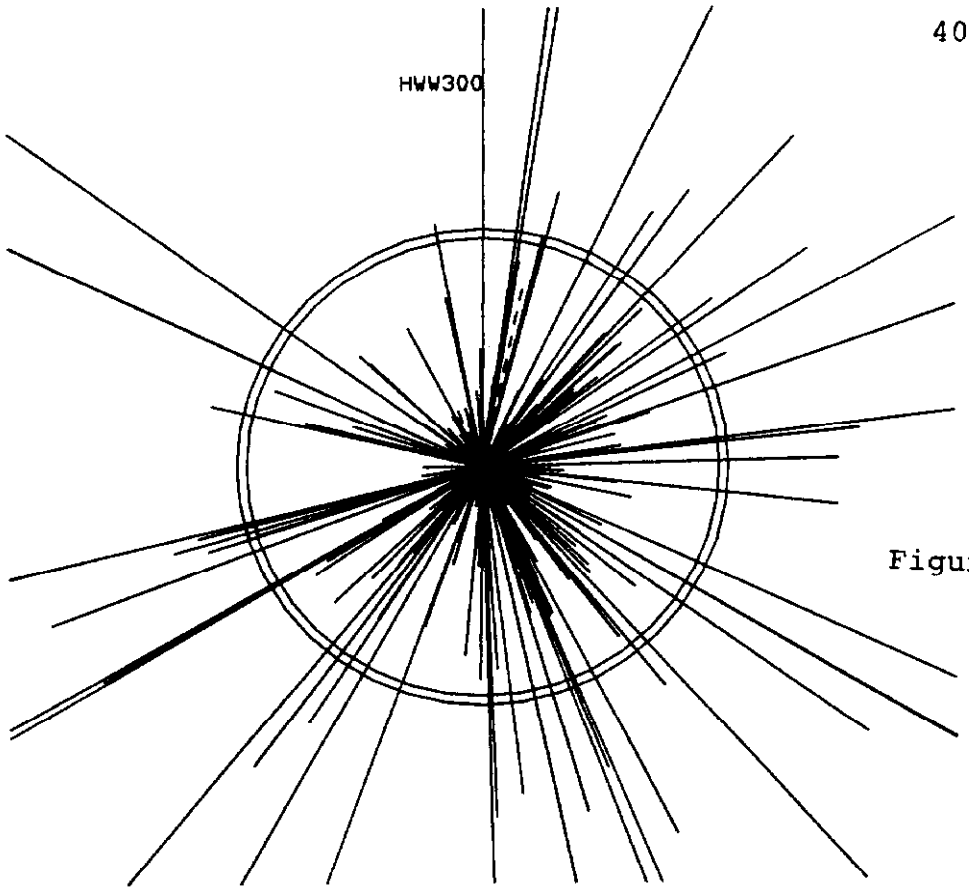

Figure 4.5 (d)

HWW300

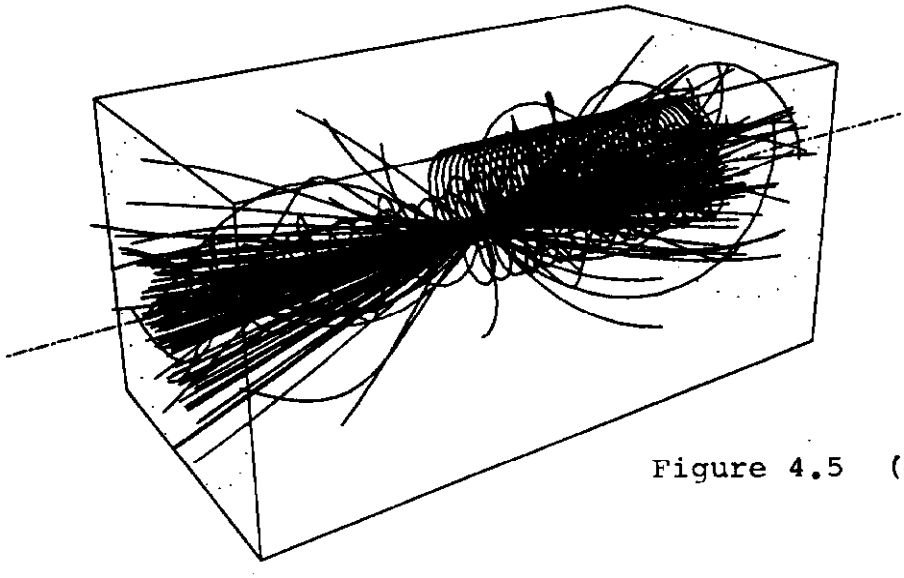

Figure 4.5 (e)

HZZ300

ID	TK	PT	PZ	P	THET	PHI
Z0	P 1	66.9	-293.1	300.6	167.1	46.2
Z0	P 2	179.4	-869.5	887.8	168.3	149.2

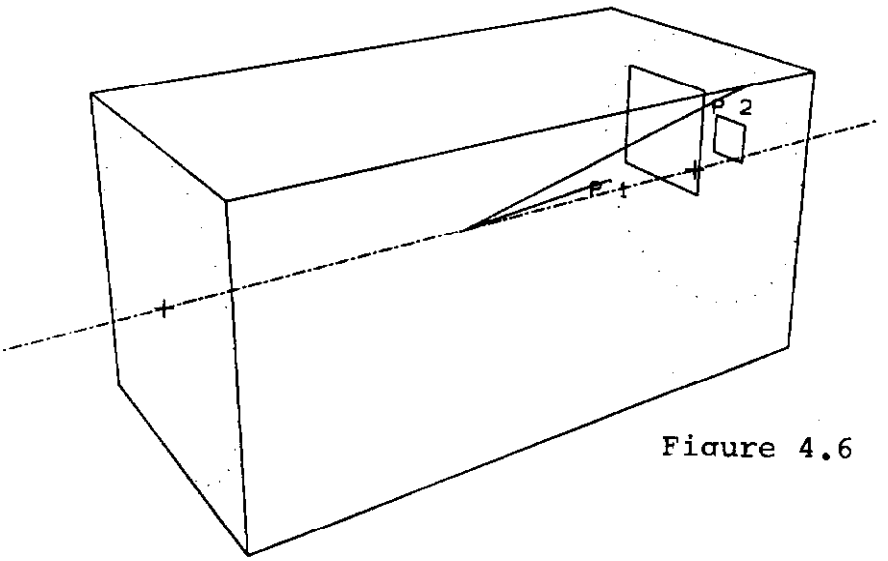

Figure 4.6 (a)

HZZ300

ID	TK	PT	PZ	P	THET	PHI
	J 1	146.2	-513.5	533.9	164.1	137.6
	J 2	111.2	423.6	438.0	14.7	-54.9
	J 3	101.2	901.7	907.4	6.4	-23.7
	J 4	53.3	-103.7	116.6	152.8	-137.7
	J 5	50.4	-368.2	371.6	172.2	-173.7
	J 6	49.5	-139.2	147.8	160.4	13.9
	J 7	47.7	-118.2	127.4	158.0	55.0
	J 8	14.3	135.8	136.5	6.0	-162.4

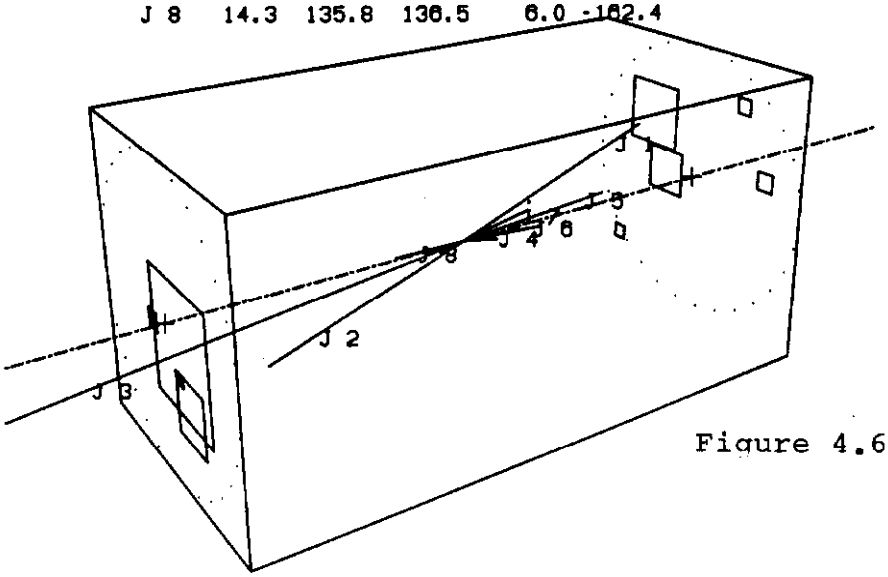

Figure 4.6 (b)

HZZ300

ID	TK	PT	PZ	P	THET	PHI
NUM	1	76.7	-149.2	167.8	152.8	69.9
ANUM	2	31.1	-143.9	147.2	167.8	-49.9
E-	3	49.6	-360.9	364.3	172.2	-172.8
E+	4	143.6	-508.6	528.5	164.2	136.9
NUT	205	52.4	-108.7	120.7	154.3	-175.9
ANUT	314	3.5	-4.1	5.4	139.4	-148.3
NUE	332	5.6	-19.0	19.8	163.5	46.5
E+	333	1.4	-4.4	4.6	161.7	19.2
	MISS	43.9				

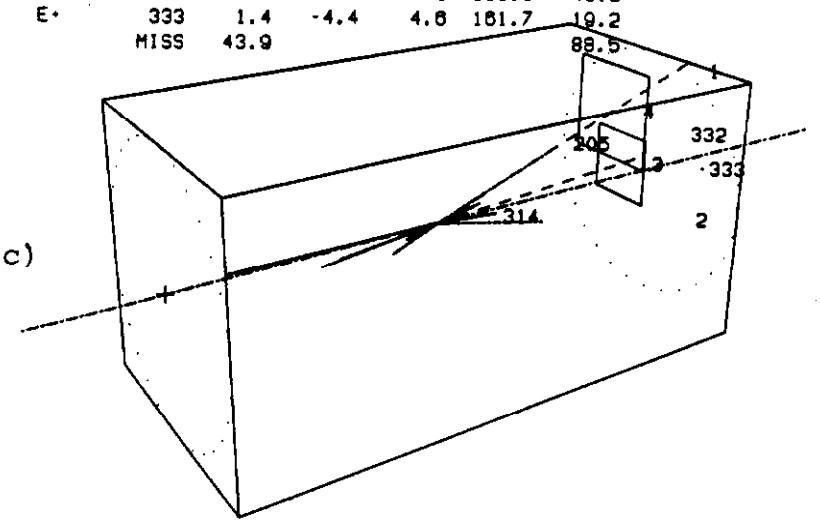

Figure 4.6 (c)

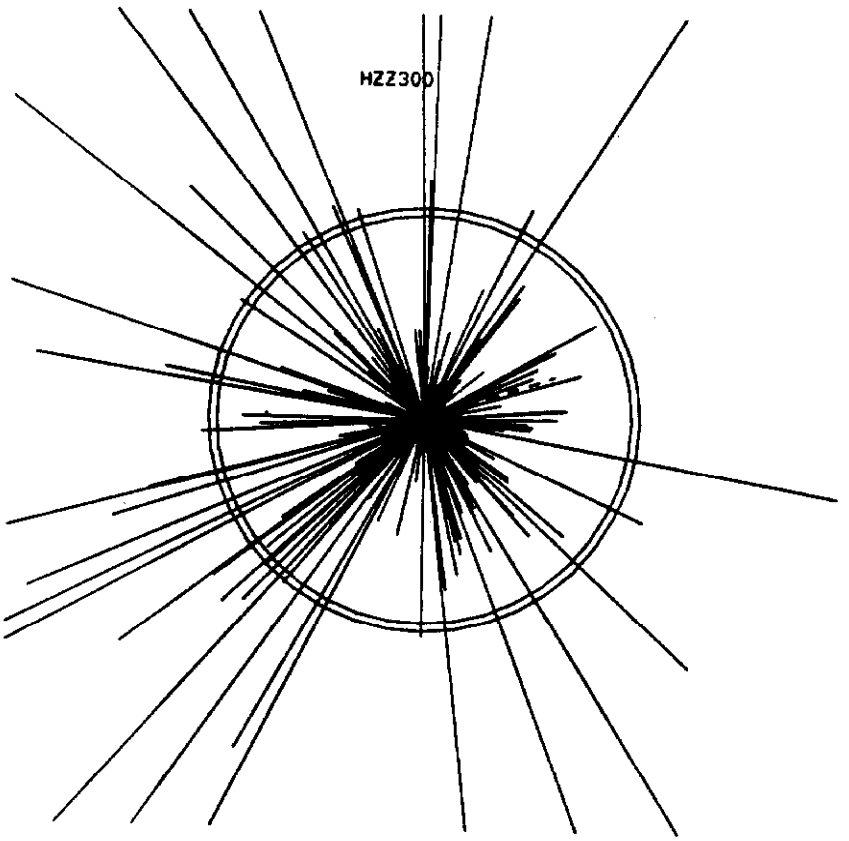

Figure 4.6 (d)

HZZ300

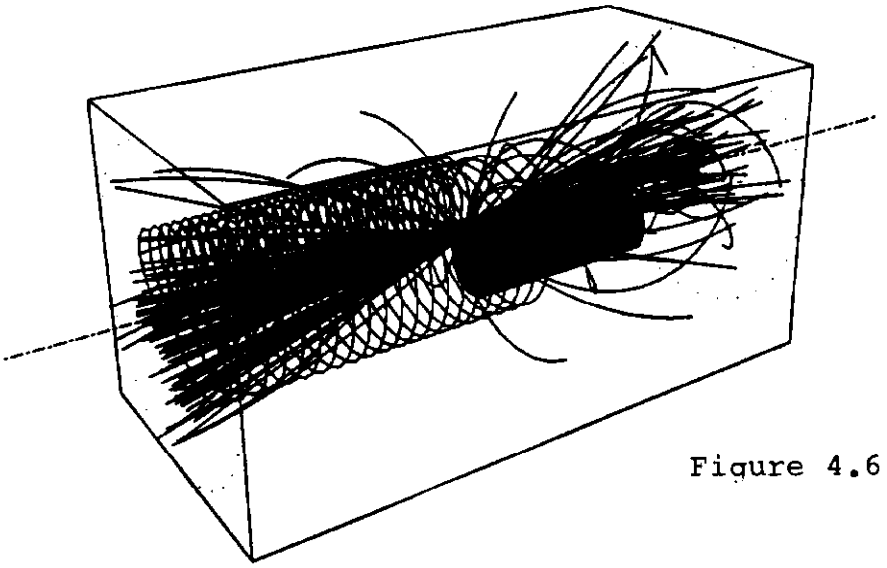

Figure 4.6 (e)

HWW800

	ID	TK	PT	PZ	P	THET	PHI
W-		P 1	283.1	308.2	418.5	42.6	-129.1
W-		P 2	533.8	275.9	600.9	62.7	50.0

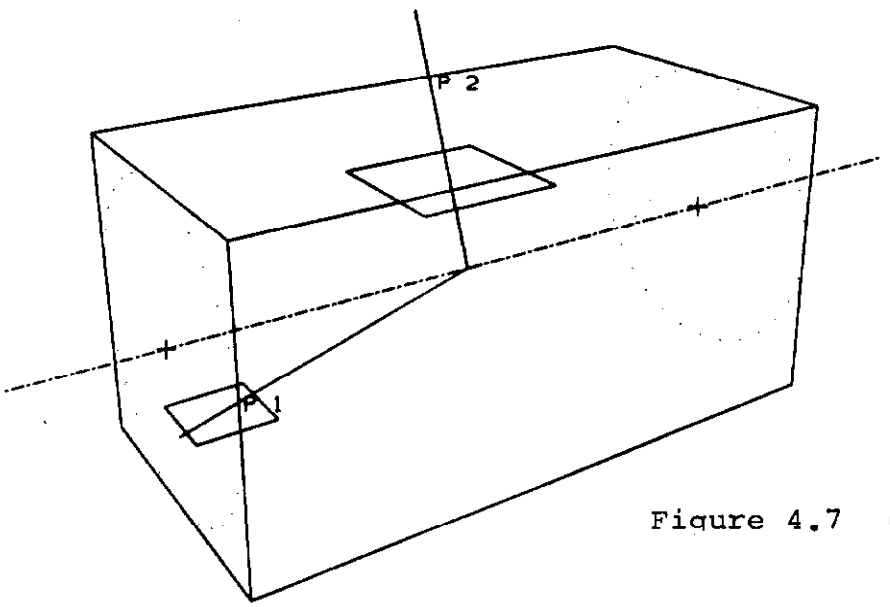

Figure 4.7 (a)

HWW800

ID	TK	PT	PZ	P	THET	PHI
	J 1	520.4	276.2	589.2	62.0	50.0
	J 2	134.5	-404.7	426.5	161.6	-129.4
	J 3	79.4	93.9	123.0	40.2	-102.3
	J 4	70.4	66.5	96.9	46.6	161.3
	J 5	35.2	-269.6	271.9	172.6	-89.1
	J 6	28.1	-60.9	67.0	155.2	-101.6
	J 7	26.1	-182.3	184.1	171.8	-7.9
	J 8	25.9	33.4	42.3	37.8	-152.6

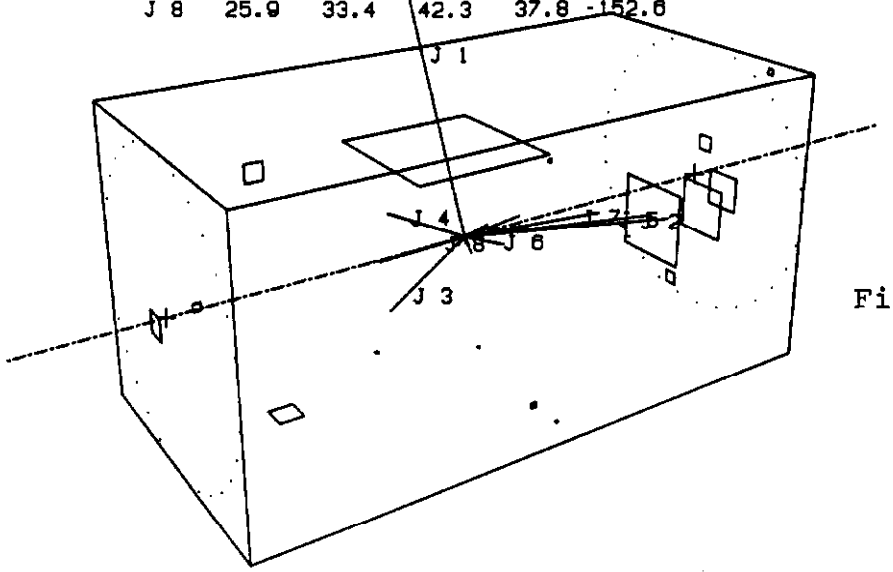

Figure 4.7 (b)

HWW800

ID	TK	PT	PZ	P	THET	PHI
MU-	1	76.5	89.4	117.7	40.6	-101.6
NUM	2	218.2	218.8	309.0	44.9	-138.4
ANUM	431	14.0	-43.4	45.6	162.1	-132.6
MU-	432	58.7	-173.9	182.9	161.9	-131.7
E-	435	12.8	9.7	16.1	52.7	159.0
ANUE	436	4.8	3.8	6.1	51.2	163.5
	MISS	241.4				-139.0

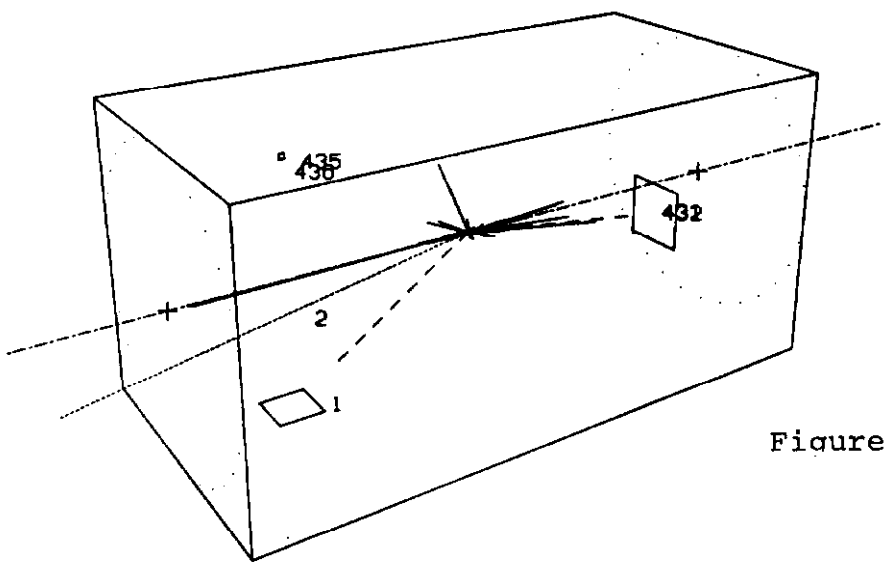

Figure 4.7 (c)

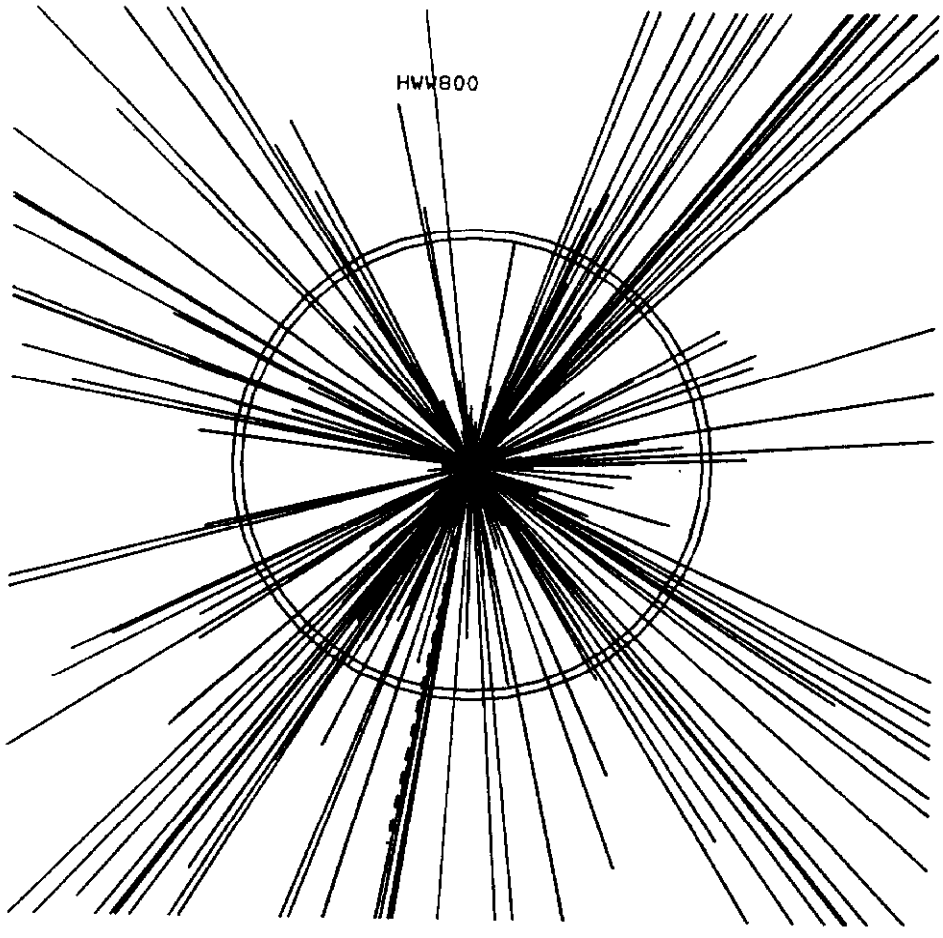

Figure 4.7 (d)

HWW800

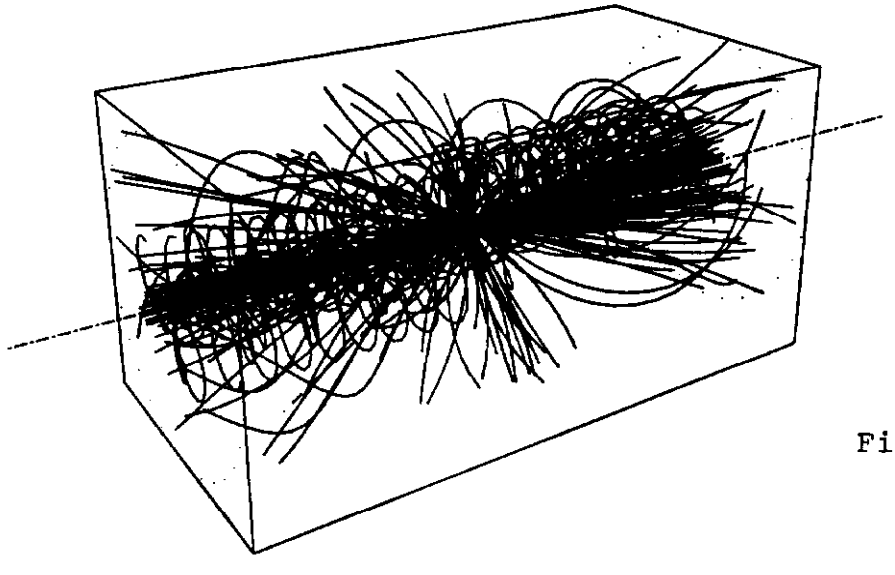

Figure 4.7 (e)

HZZ800

ID	TK	PT	PZ	P	THET	PHI
ZO	P 1	812.4	-746.7	1103.4	132.6	-109.9
ZO	P 2	787.9	-2133.7	2274.5	159.7	63.0

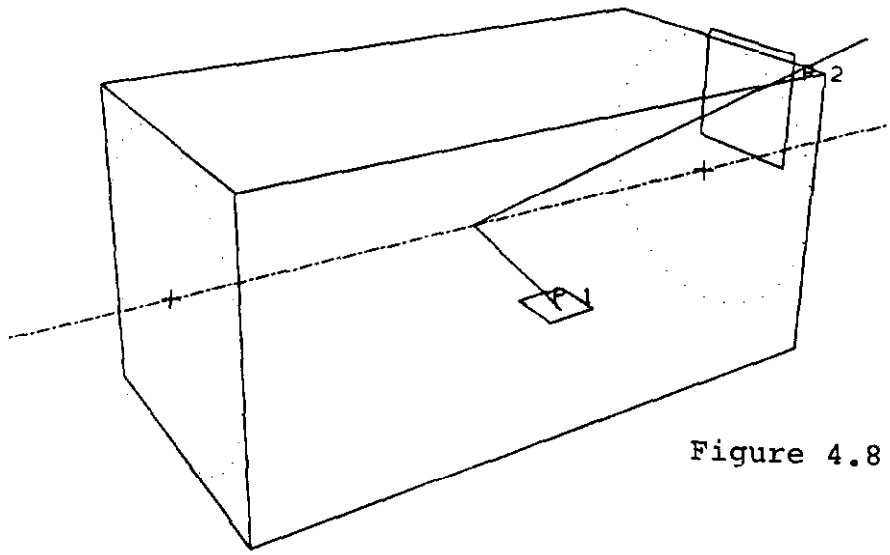

Figure 4.8 (a)

HZZ800

ID	TK	PT	PZ	P	THET	PHI
	J 1	801.1	-2193.9	2335.6	159.9	62.7
	J 2	102.5	-920.3	926.0	173.6	-139.7
	J 3	33.6	-278.6	280.6	173.1	-12.1
	J 4	29.9	-18.3	35.1	121.4	70.3

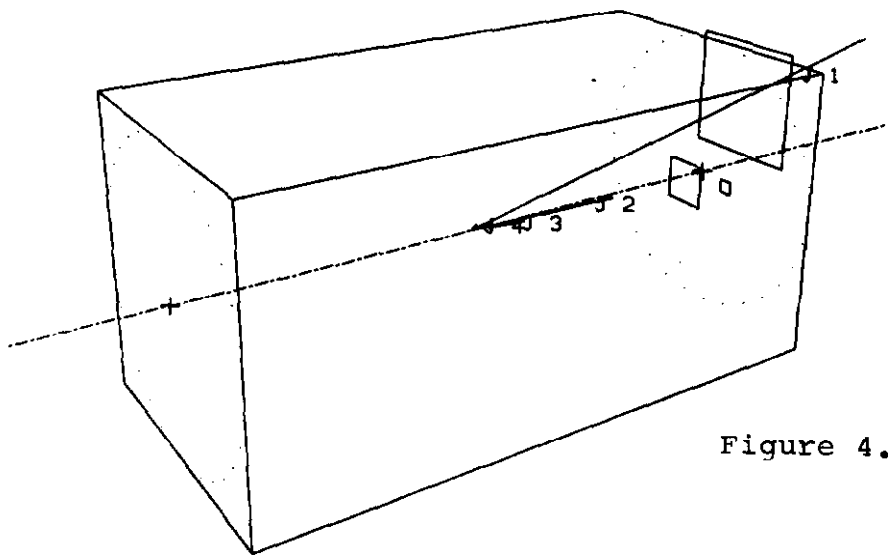

Figure 4.8 (b)

HZZ800

ID	TK	PT	PZ	P	THET	PHI
NUM	1	223.5	-183.7	289.3	129.4	-120.0
ANUM	2	593.6	-563.0	818.1	133.5	-106.2
MU-	3	347.9	-976.3	1036.5	160.4	70.3
MU+	4	445.1	-1157.3	1239.9	159.0	57.2
NUT	94	100.5	-119.9	156.5	140.0	82.3
E-	111	0.2	-3.8	3.8	177.6	155.6
NUE	148	16.5	-13.4	21.2	129.0	71.6
E+	149	7.4	-5.3	9.0	125.6	75.4
	MISS	660.1				-112.3

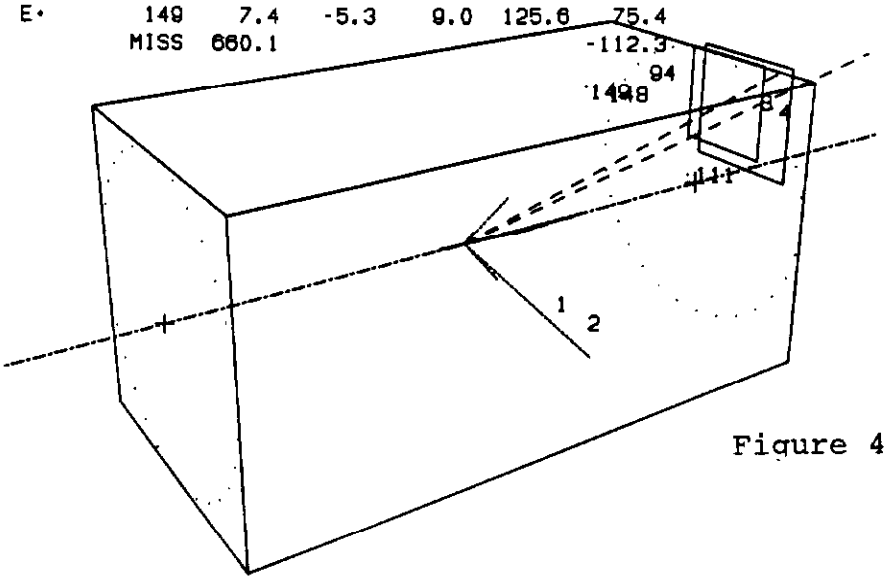

Figure 4.8 (c)

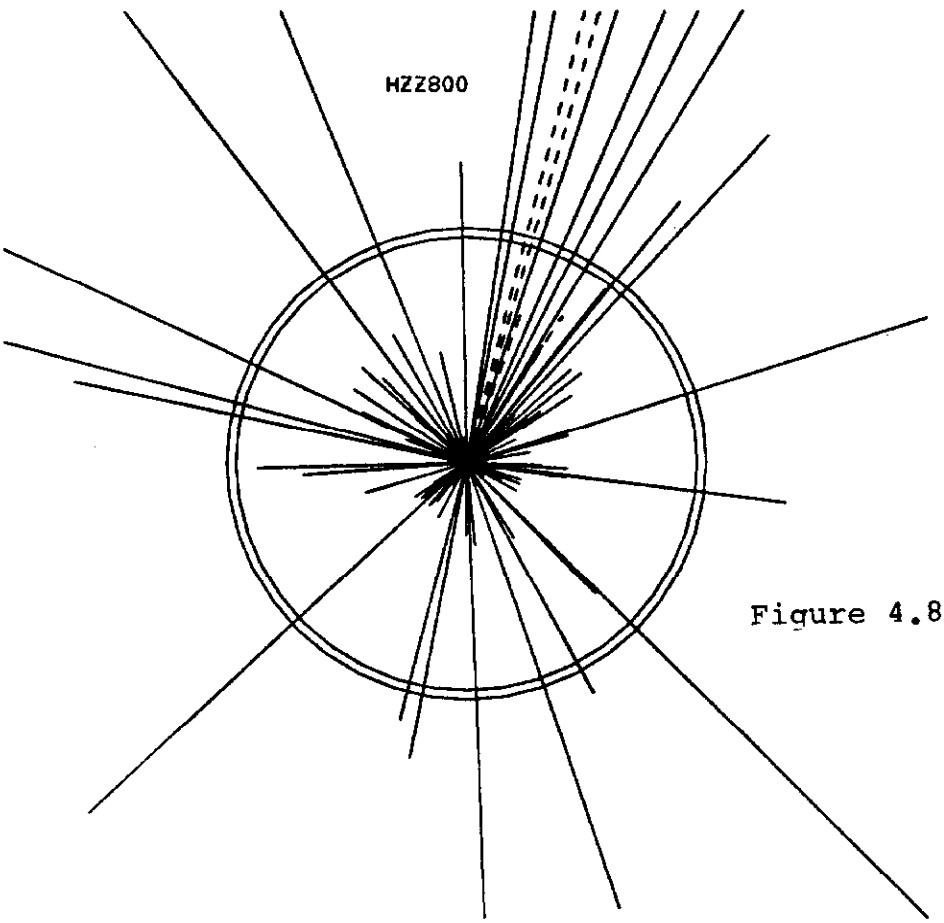

Figure 4.8 (d)

HZZ800

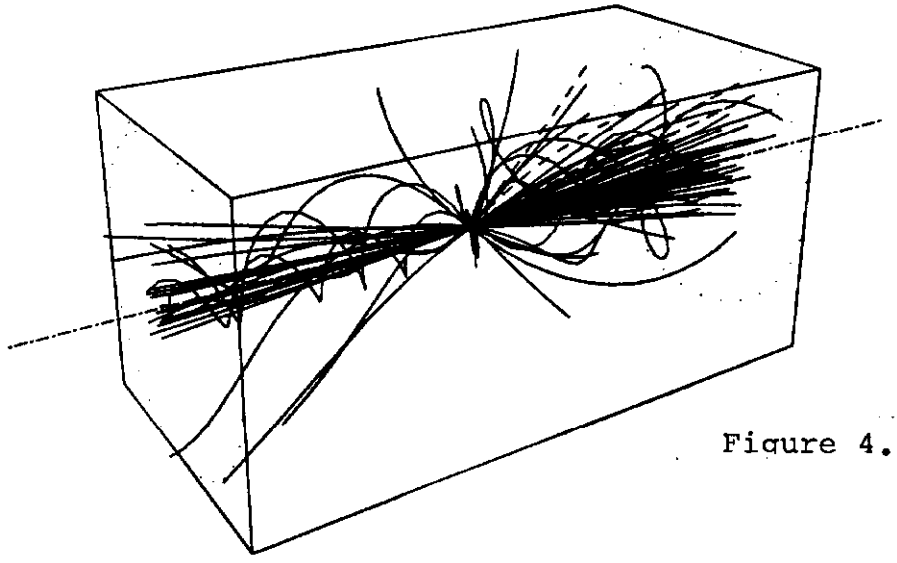

Figure 4.8 (e)

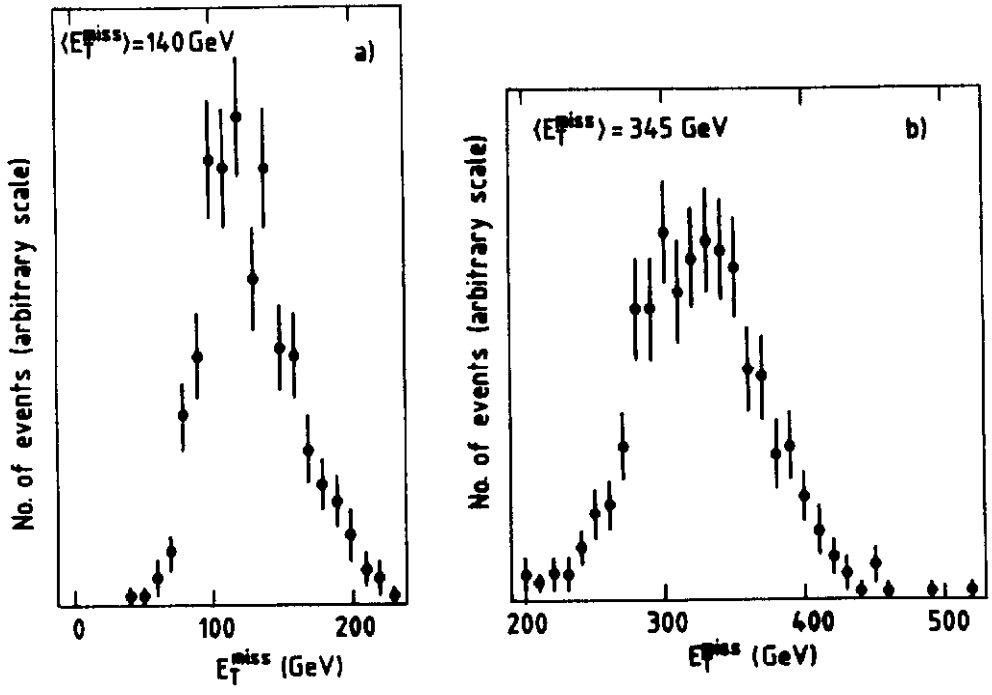

Figure 4.9

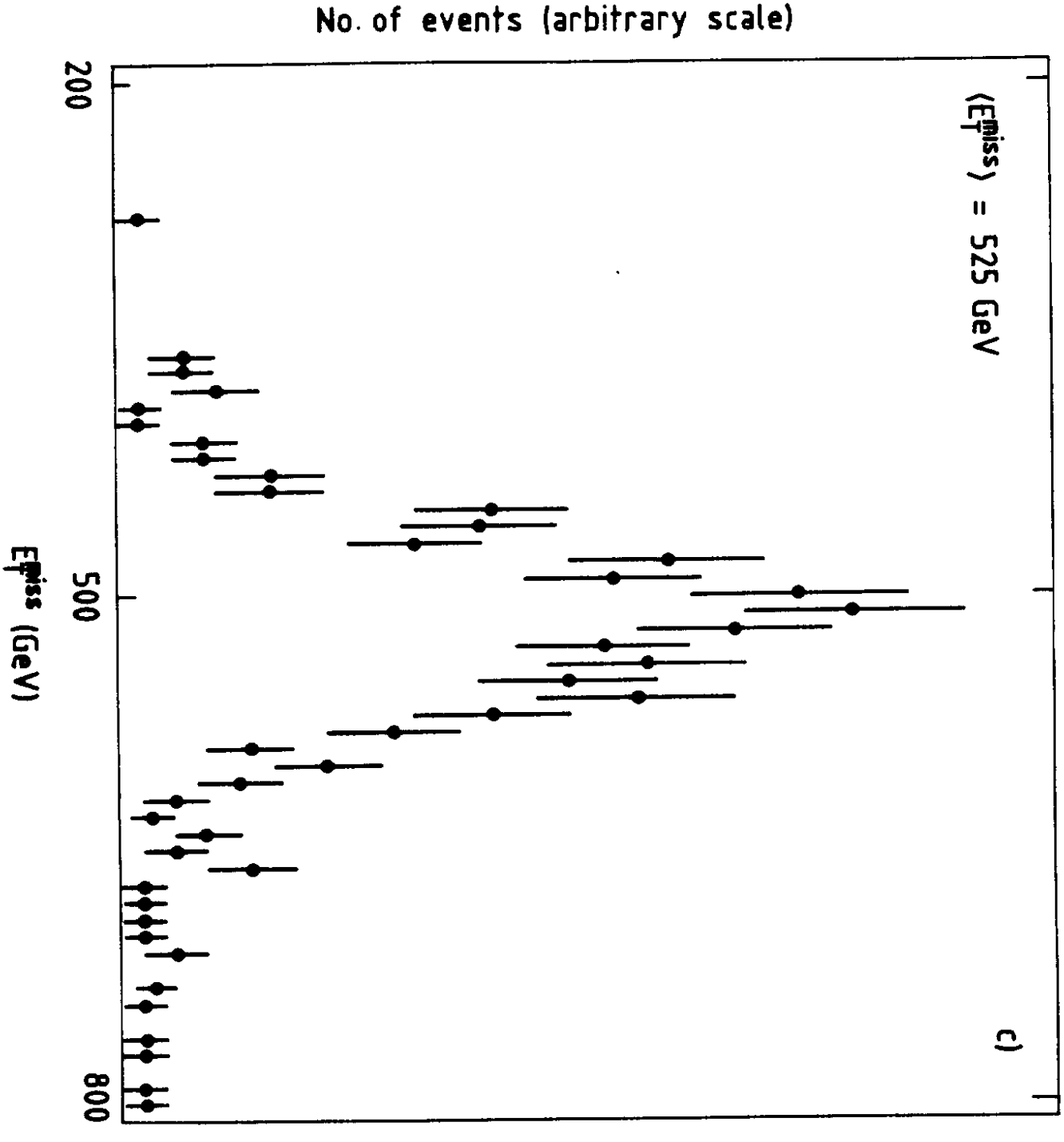
No. of events (arbitrary scale)
200
500
800
E_T^{miss} (GeV)
(E_T^{miss}) = 525 GeV
c)

Figure 4.9

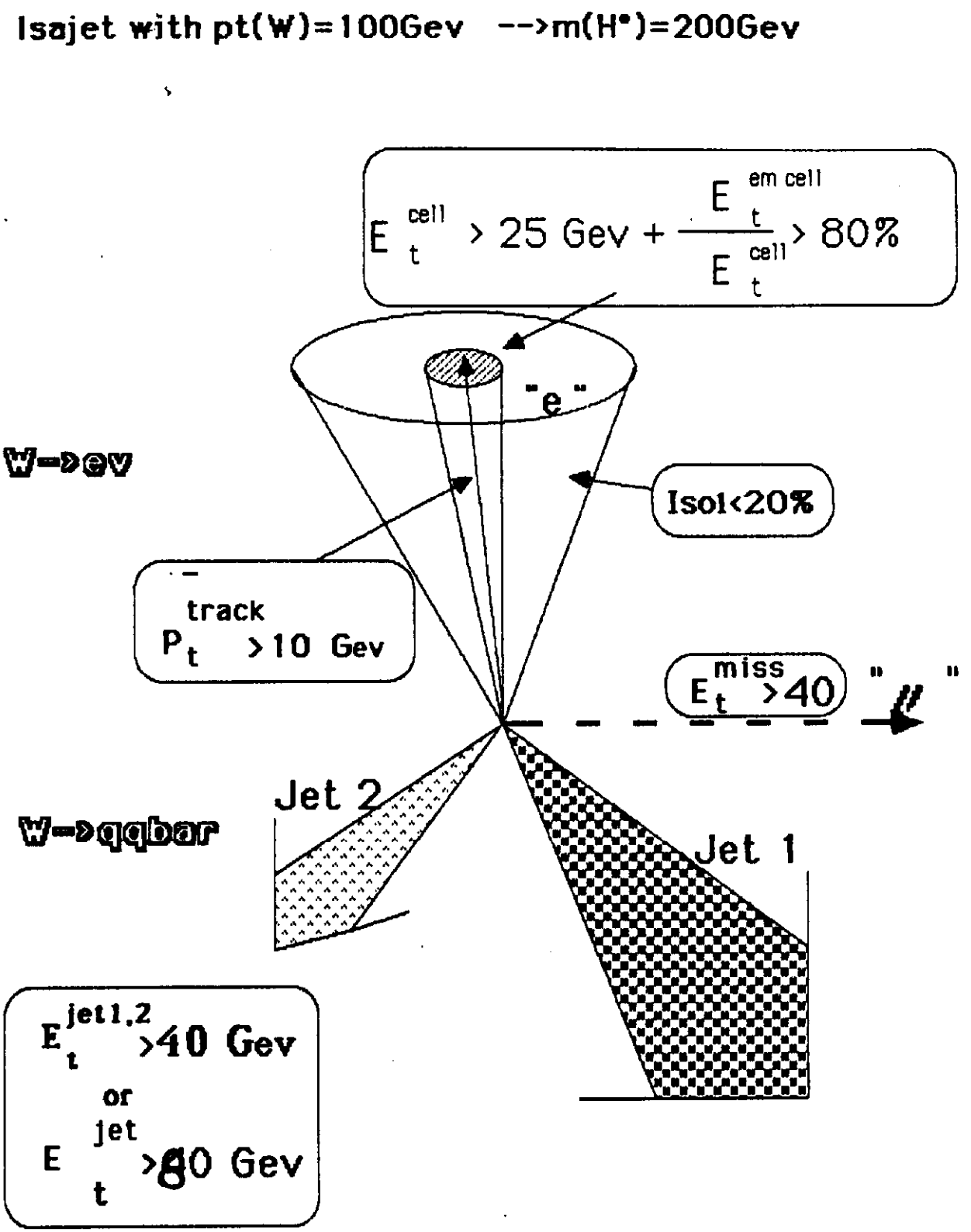
Isajet with pt(W)=100Gev -->m(H°)=200Gev
$E_t^{cell} > 25\ Gev + \frac{E_t^{em\ cell}}{E_t^{cell}} > 80\%$
"e"
W->ev
Isol<20%
$P_t^{track} > 10\ Gev$
$E_t^{miss} > 40$
"ν"
Jet 2
W->qqbar
Jet 1
$E_t^{jet1,2} > 40\ Gev$
or
$E_t^{jet} > 80\ Gev$

Figure 4.10